Partial Reconstruction of Black Hole Thermodynamic Geometry from Horizon Residues

Wen-Xiang Chen
wxchen4277@qq.com

School of Electronic Information, Guangzhou City University of Technology,
Guangzhou, China

Abstract

How much of a black hole's thermodynamic geometry can be inferred from its Hawking temperature? We consider static, spherically symmetric black holes whose analytic metric functions have simple zeros at the outer horizon. With a common normalization of Killing time, the residue b of the radial optical one-form gives $T = (4\pi b)^{-1}$ for each member of the family. At fixed pressure and with the entropy specified, the field $b(S, Q)$ determines one row of the entropy metric, including the inverse heat capacity $C_{Q,P}^{-1} = -\partial_S \log b$. The remaining entry depends on $F''(Q)$, where $F(Q)$ is the enthalpy on one reference isentrope. We exhibit two locally stable thermodynamic potentials with identical temperature fields and different scalar curvatures. Four-dimensional charged anti-de Sitter black holes exhibit two distinct pole collisions along fixed-charge isobars. At the canonical critical pressure P_c, the heat capacity has a double pole in the horizon radius and the ordinary entropy curvature is finite. At $3P_c$, the isobar touches the metric-degeneracy locus quadratically. The curvature then has a fourth-order pole at finite heat capacity. Analytic continuation tracks the two spinodal radii into the complex plane with their total multiplicity intact. Phase coexistence requires a separate comparison of the free energies at two real radii with the same temperature.

Keywords black hole thermodynamics, horizon residues, thermodynamic geometry, heat capacity, spinodals, charged AdS black holes

1 Introduction

At fixed nonzero charge, the heat capacity of an asymptotically flat Reissner–Nordström (RN) black hole diverges when the squared outer horizon radius equals three times the squared charge. Its two-variable entropy metric is flat there. To see how these two statements fit together, consider the information available at a horizon. A radial derivative within one spacetime sets its Hawking temperature. To obtain the heat capacity, one varies the mass at fixed charge and compares the temperatures of nearby equilibria. A curvature calculation also requires information about variations in charge. We use the optical residue to identify exactly which of these variations the temperature field determines.

The normalization of T and S used here follows from black-hole mechanics, the entropy–area relation and Hawking's calculation of particle creation [1–3]. Both the propagator and Euclidean derivations of the temperature use analyticity at the horizon [4, 5]. In tunneling calculations the corresponding choice is the path taken across the horizon [6–8]. Robson, Villari and Biancalana (RVB) obtained the temperature from the topology of the two-dimensional Euclidean section [9]. The local contour description isolates the coefficient of a simple pole in the radial optical one-form [10, 13]. Applications include charged and rotating black holes in modified gravity [11, 12]. For the quadratic $f(Q)$ solution studied in Ref. [13], the same coefficient gives the logarithmic term in the scalar tortoise coordinate. To recover entropy one must also supply a first law and its integration data, or a normalized Noether charge [1, 14, 15, 35, 36].

The choice of thermodynamic metric matters even for the RN family. Weinhold's energy Hessian and Ruppeiner's negative entropy Hessian each refer to the natural variables of the corresponding potential [16–18]. The ordinary entropy metric is flat for asymptotically flat RN black holes and can have singular curvature in anti-de Sitter (AdS) space [19]. Davies identified poles in the heat capacities of charged and rotating black holes [20]. Whether a thermodynamic curvature also diverges at such a pole depends on the potential [21–23] and on which variables the ensemble allows to fluctuate [24, 25]. Other choices include a Legendre-invariant metric [26], and the choice arises in charged solutions of modified gravity as well [27]. Here we form the negative entropy Hessian in (M, Q) at fixed pressure and transform it to (S, Q) as a tensor.

Several complex-variable descriptions of black-hole phases start from a free energy. They count defects of an off-shell potential [28], express their winding numbers as residues [29], or follow zeros of a free-energy derivative into the complex plane [30–32]. Real temperature extrema also enter counts of equilibrium branches and their relation to complex foliations [33]. The closest antecedent for our charged-AdS calculation is the spinodal polynomial of Xu and Mann, who continued its roots away from the real radius axis [34].

Scope and main results

The residue calculations of Refs. [11–13] recover the temperature for a given horizon. Ref. [15] connects this local result to Euclidean regularity and Noether-charge normalization and examines its implications for gravitational dynamics. Here the unknown is the thermodynamic metric. We assume a static, spherically symmetric family with a nondegenerate outer horizon, analytic metric functions and the same Killing-time normalization across the family. On a fixed-pressure patch with an independently specified entropy, the residue fixes the entropy row of the metric. Section 4 identifies the remaining datum as the charge dependence of the enthalpy on a single isentrope. An explicit pair of locally stable potentials gives different curvatures for the same temperature field. This example lies within analytic thermodynamics. A black-hole realization would require a solution of the gravitational field equations.

For four-dimensional RN–AdS we can compare the canonical spinodal polynomial [34, 45] with the degeneracy condition for the ordinary entropy metric [19] on the same family. Each condition becomes a quadratic in the squared horizon radius at fixed charge. Their discriminants vanish at different pressures. At P_c two heat-capacity poles merge. At $3P_c$ a fixed-charge isobar is tangent to the metric-degeneracy locus. Equations (3.18) and (3.19) give the orders and leading coefficients of the resulting poles. The factor of three between these pressures comes from the RN–AdS equation of state.

2 The horizon residue and its variation across equilibria

2.1 The optical residue and the Euclidean period

Use units $G = \hbar = c = k_{\mathrm{B}} = 1$. For a static, spherically symmetric black hole with fixed Killing time t and areal radius w, the exterior metric reads

$$ds^2 = -A(w)\,dt^2 + \frac{dw^2}{B(w)} + w^2 d\Omega_2^2. \tag{2.1}$$

Assume that A and B are real analytic near the outer horizon $w = h$, where both vanish linearly with slopes $a_1, b_1 > 0$. Writing $\xi = w - h$, we have $A = a_1\xi + a_2\xi^2 + O(\xi^3)$ and $B = b_1\xi + b_2\xi^2 + O(\xi^3)$. On a disk small enough that the remaining factors have no zeros, factor $a_1 b_1 \xi^2$ from the product and choose the branch positive in the exterior,

$$\sqrt{AB} = \sqrt{a_1 b_1}\,\xi \left[1 + \frac{1}{2}\left(\frac{a_2}{a_1} + \frac{b_2}{b_1}\right)\xi + O(\xi^2)\right]. \tag{2.2}$$

On this branch radial null rays obey $dt = \pm dw/\sqrt{AB}$. The radial optical one-form hence has a simple pole,

$$\omega = \frac{dw}{\sqrt{AB}} = b\left[\frac{1}{\xi} - \frac{1}{2}\left(\frac{a_2}{a_1} + \frac{b_2}{b_1}\right) + O(\xi)\right] d\xi, \tag{2.3}$$

$$b = \operatorname*{Res}_{w=h} \omega = \frac{1}{2\pi i}\oint_{\gamma_h} \omega = \frac{1}{\sqrt{a_1 b_1}}. \tag{2.4}$$

Here γ_h winds once counterclockwise around h and encloses no other pole. A single spacetime supplies one value of b. Across a family of equilibria, these values define a field on state space. The term $b\log\xi$ in a primitive of ω increases by $2\pi i b$ in one circuit. The residue of $d\log A$ counts the multiplicity of the zero, here unity since $A = \xi(a_1 + O(\xi))$. For example, the Schwarzschild metric function in Eq. (4.6) of Ref. [10] vanishes linearly at $w = 2M$. Its reciprocal multiplied by dw has a pole whose residue carries units of length.

On the Euclidean section, set $t = -i\tau$ and $\rho = 2\sqrt{\xi/b_1}$. Substitution of $\xi = b_1\rho^2/4$ and $d\xi = (b_1\rho/2)d\rho$ gives $d\xi^2/B = [1 + O(\rho^2)]d\rho^2$ and $A\,d\tau^2 = (a_1 b_1/4)\rho^2[1 + O(\rho^2)]d\tau^2$. Smoothness at $\rho = 0$ requires the polar angle $\sqrt{a_1 b_1}\,\tau/2$ to have period 2π. This fixes the surface gravity and thermal period in the chosen time coordinate,

$$\kappa = \tfrac{1}{2}\sqrt{a_1 b_1}, \qquad \beta = \frac{2\pi}{\kappa} = 4\pi b, \qquad T_H = \frac{1}{4\pi b}. \tag{2.5}$$

On the real exterior branch, β is twice the magnitude of the optical monodromy [5, 15]. For Schwarzschild, $A = B = 1 - 2M/w$ and $\omega = (1 + 2M/(w - 2M))dw$. Its residue $b = 2M$ yields the usual $T_H = 1/(8\pi M)$.

The Gauss–Bonnet construction recovers this period in Schwarzschild gauge $A = B = f$ [9]. Truncate the Euclidean orbit-space disk at $w = L > h$, within the static region $f > 0$. Its metric has unit determinant, and the Christoffel symbols $\Gamma^w_{\tau\tau} = -ff'/2$, $\Gamma^\tau_{w\tau} = f'/(2f)$, and $\Gamma^w_{ww} = -f'/(2f)$ give the scalar curvature $R^{(2)} = -f''$. The bounding circle has line element $ds = \sqrt{f(L)}d\tau$. With the induced boundary orientation its geodesic curvature obeys $k_g\,ds = f'(L)d\tau/2$. The Euler characteristic of the disk is therefore

$$1 = \frac{\beta}{4\pi}\int_h^L [-f''(w)]\,dw + \frac{\beta}{4\pi}f'(L) = \frac{\beta f'(h)}{4\pi}. \tag{2.6}$$

The boundary term cancels the bulk contribution at L. Only the horizon slope $f'(h) = 1/b$ enters the period. The disk argument requires a Euclidean period smooth at every horizon it describes. It fails when those periods are incompatible.

2.2 A family of solutions with a common Killing time

Let z label equilibrium solutions at fixed work variables. Within each spacetime, w denotes radius and $h(z)$ the simple horizon. Assume holomorphic dependence on z. Use a common, future-directed normalization of Killing time and choose the branch with $T > 0$ on the real slice. For z near its base value, a single circle γ in the w-plane continues to enclose the moving horizon alone. Write the optical denominator as $(w - h(z))\,U(w, z)$, where U is holomorphic and nonzero near the horizon. Evaluating the residue and differentiating with respect to z gives

$$b(z) = \frac{1}{2\pi i}\oint_\gamma \omega(w; z) = \frac{1}{U(h(z), z)}, \qquad b'(z) = -\frac{U_w(h, z)h'(z) + U_z(h, z)}{U(h, z)^2}. \tag{2.7}$$

Here $U_w h'$ accounts for the motion of the horizon and U_z for the variation of U at fixed radius. In logarithmic derivatives we write $\log b$ for $\log(b/b_{\mathrm{ref}})$, with a fixed nonzero reference length b_{ref}. A holomorphic radial coordinate change with nonzero Jacobian leaves the contour integral invariant. A common rescaling of Killing time multiplies each residue by a constant, preserving

$d \log b$. A state-dependent factor contributes its own logarithmic derivative. Equation (2.7) uses the holomorphic branch selected at the real base point. Taking the modulus would lose holomorphicity.

Let M and an independently normalized entropy obey $dM = T\,dS$ at fixed work variables, with $T = T_H$. On a simply connected regular patch, substituting Eq. (2.5) into the first law and integrating gives

$$S(z) - S(z_0) = 4\pi \int_{z_0}^{z} b(\zeta) M'(\zeta)\, d\zeta. \tag{2.8}$$

The integral requires $M'(z)$ along the family. Its value gives an entropy difference. The absolute entropy also requires a reference value $S(z_0)$ [14]. Allowing charge and pressure to vary gives the entropy one-form $T^{-1}(dM - \Phi\, dQ - V\, dP)$. If this form is closed, a local entropy exists. A global single-valued entropy further requires its periods around noncontractible cycles to vanish. In Einstein gravity the action fixes the area normalization. For a diffeomorphism-covariant higher-curvature Lagrangian, the Wald Noether charge fixes the entropy at a stationary bifurcate Killing horizon [35, 36]. The contour winding carries no entropy normalization.

At fixed work variables, take $S'(z) \neq 0$ so that entropy serves as a local coordinate. The derivative of $4\pi bT = 1$, together with $dT/dS = T'/S'$, then determines the heat capacity,

$$\frac{T'}{T} = -\frac{b'}{b}, \qquad \frac{1}{C} = \frac{1}{T}\frac{T'}{S'} = -\frac{b'}{bS'}, \qquad C = -\frac{bS'}{b'}. \tag{2.9}$$

These identities extend meromorphically with the state functions, provided T' does not vanish identically. An isolated zero of b' is a regular point of $1/C$ when $bS' \neq 0$. For Schwarzschild, take $z = 2M$, so that $S = \pi z^2$ and $b = z$. Equations (2.9) and (2.8) yield $C = -2\pi z^2 = -8\pi M^2$ and $dS = 2\pi z\, dz$, respectively. This negative heat capacity applies to the unconfined solution. In a finite thermal cavity the boundary temperature changes, as does the stability criterion [37].

2.3 Coalescing horizons in the extremal RN limit

The asymptotically flat RN metric has $f(w) = (w - r_+)(w - r_-)/w^2$, where $r_\pm = M \pm \sqrt{M^2 - Q^2}$. While the two horizons are distinct, $r_+ > r_-$, a partial fraction expansion of $dw/f(w)$ gives

$$b_+ = \frac{r_+^2}{r_+ - r_-}, \qquad b_- = -\frac{r_-^2}{r_+ - r_-}, \qquad b_+ + b_- = r_+ + r_-. \tag{2.10}$$

As the horizons approach $r_e = |Q| > 0$, the outer residue b_+ diverges to $+\infty$ and T_H tends to zero. Setting the roots equal before expanding gives a different Laurent series,

$$\omega = \left[\frac{r_e^2}{(w - r_e)^2} + \frac{2r_e}{w - r_e} + 1\right] dw. \tag{2.11}$$

A contour enclosing both poles throughout the merger measures $b_+ + b_-$, which tends to the extremal residue $2r_e$. A contour isolating the outer horizon before coalescence measures the divergent b_+. In the extremal geometry, the integral $\int dw/(w - r_e)$ in the proper radial distance diverges logarithmically, placing the extremal horizon at the end of an infinite throat. The Euclidean section has lost the finite-distance polar origin at which smoothness selected a thermal period [15, 38]. Regularity at the end of the throat supplies no conical-period condition. The zero temperature follows from the limit of the nonextremal family.

3 The entropy metric and its analytic continuation

3.1 The entropy Hessian in mass and entropy coordinates

Fix the external parameters and consider a real-analytic fundamental relation $M(S, Q)$ on an open set of equilibrium states. For an AdS black hole the pressure is held fixed, so the mass plays

the role of enthalpy. In the chart $x = (S, Q)$, the first law identifies $T = M_S$ and $\Phi = M_Q$. Two Hessians enter the geometry, one formed from M in this chart and the other from the entropy in the chart $y = (M, Q)$,

$$W_{ij} = \frac{\partial^2 M}{\partial x^i \partial x^j}, \qquad g^{(y)}_{ab} = -\frac{\partial^2 S}{\partial y^a \partial y^b}. \tag{3.1}$$

The choice of potential thus specifies the variables in which the second derivatives must be taken [16–19]. To describe equilibrium fluctuations, the resulting metric must be positive definite on the real variations admitted by the ensemble.

When $T \neq 0$, the inverse function theorem gives a local entropy function $S(M, Q)$. At fixed charge its mass derivative is $S_{,M} = 1/T$, while at fixed mass its charge derivative is $S_{,Q}|_M = -\Phi/T$. Composing S with $y(x)$ recovers the coordinate x^1, whose second derivatives vanish. The chain rule then gives

$$0 = S_{,ab} y^a{}_{,i} y^b{}_{,j} + S_{,a} y^a{}_{,ij} = S_{,ab} y^a{}_{,i} y^b{}_{,j} + \frac{1}{T} M_{,ij}. \tag{3.2}$$

Only the mass coordinate can contribute second derivatives in this change of variables, since $y^2 = Q$. Pulling back the negative entropy Hessian to (S, Q) therefore gives

$$g_{ij} = g^{(y)}_{ab} y^a{}_{,i} y^b{}_{,j} = \frac{W_{ij}}{T}. \tag{3.3}$$

This relation determines the metric in any subsequent chart by the tensor transformation law. Differentiating M twice with respect to new coordinates after a nonlinear change would introduce an extra term $M_{,i}\, \partial_\alpha \partial_\beta x^i$.

Real analyticity also fixes the complex continuation near each interior point. In a sufficiently small complex polydisc, the Taylor expansion of M converges to a holomorphic germ $\mathcal{M}(z^1, z^2)$. The real derivatives at the chosen point fix its Taylor coefficients, so the germ is unique. Differentiating the same series defines

$$\mathcal{T} = \partial_1 \mathcal{M}, \qquad \mathcal{W}_{ij} = \partial_i \partial_j \mathcal{M}, \qquad \}_{ij} = \frac{\mathcal{W}_{ij}}{\mathcal{T}}. \tag{3.4}$$

On the set $\mathcal{T} \det \mathcal{W} \neq 0$, $\}$ is a holomorphic, nondegenerate symmetric complex-bilinear form. Its determinant is $\det \} = \det \mathcal{W}/\mathcal{T}^2$, and its inverse is $\}^{-1} = \mathcal{T}\, \mathrm{adj}(\mathcal{W})/\det \mathcal{W}$. Both the connection and the curvature are holomorphic there and admit meromorphic continuations on the polydisc when neither denominator is identically zero. To locate an actual pole one must cancel the common factors of numerator and denominator. If the coordinates involve a square root, the change of chart is valid locally on a biholomorphic branch. Positivity is a condition on the real slice.

At fixed charge the only variation available to the heat capacity is the entropy variation. Where $T \neq 0$, that response and the determinant of the unrestricted Hessian take the forms

$$C_Q = T \left(\frac{\partial S}{\partial T} \right)_Q = \frac{T}{M_{SS}}, \qquad \det W = M_{SS} M_{QQ} - M_{SQ}^2. \tag{3.5}$$

At a zero of M_{SS} with $M_{SQ} \neq 0$, the determinant reduces to $-M_{SQ}^2$. The fixed-charge response can diverge at such a point while the full metric remains nonsingular. Its determinant is negative on the real slice at this point, so allowing charge fluctuations gives an indefinite quadratic form.

3.2 The fixed-pressure metric of a charged Einstein–Maxwell black hole

For the four-dimensional Einstein–Maxwell family, the outer horizon radius r parametrizes equilibrium states at a given charge. Write $a = 8\pi P = 3/\ell^2$ in AdS and set $a = 0$ in the

asymptotically flat limit. Setting $1-2M/r+Q^2/r^2+ar^2/3$ to zero at the horizon and using the area law gives

$$M=\frac{r}{2}+\frac{Q^2}{2r}+\frac{ar^3}{6},\qquad S=\pi r^2,\qquad \partial_S|_Q=\frac{1}{2\pi r}\,\partial_r|_Q\,. \tag{3.6}$$

For continuation in S, take the branch of $r=\sqrt{S/\pi}$ with $r>0$ at the real base point. With $u=Q/r$, three dimensionless combinations recur in the temperature and the Hessian,

$$H=1+ar^2-u^2,\qquad D_g=-1+ar^2+u^2,\qquad K=-1+ar^2+3u^2. \tag{3.7}$$

The mass derivative at fixed charge is $M_r=H/2$. Dividing by $2\pi r$ gives $T=H/(4\pi r)$. Writing the temperature as $4\pi T=r^{-1}+ar-Q^2r^{-3}$ makes its radial derivative and the entries of the Hessian explicit,

$$\begin{aligned}&4\pi(\partial_r T)_Q=-r^{-2}+a+3Q^2r^{-4}=K/r^2,\\ &M_{SS}=\frac{K}{8\pi^2r^3},\qquad M_{SQ}=-\frac{u}{2\pi r^2},\qquad M_{QQ}=\frac{1}{r}.\end{aligned} \tag{3.8}$$

The charge derivatives follow directly at fixed entropy, where r is constant, from $M_{SQ}=(\partial_Q T)_S$ and $M_{QQ}=(\partial_Q(Q/r))_S$. The mixed entry contributes $-2u^2$ to the numerator of the determinant, changing K to D_g. The fixed-charge heat capacity follows from T/M_{SS},

$$\det W=\frac{D_g}{8\pi^2r^4},\qquad C_{Q,P}=\frac{2\pi r^2H}{K}. \tag{3.9}$$

The response functions introduced in Eqs. (5.2) and (5.3) consequently have $N(r)=r^2H$ and $D(r)=r^2K$. The quantity that tests degeneracy of the full Hessian is D_g.

The mixed terms cancel in the (r,u) chart. To see the cancellation, substitute $dS=2\pi r\,dr$ and $dQ=u\,dr+r\,du$ in $W_{SS}dS^2+2W_{SQ}\,dS\,dQ+W_{QQ}dQ^2$. The Weinhold and entropy line elements then read

$$\begin{aligned}ds^2_W&=\frac{K}{2r}\,dr^2-\frac{2u}{r}\,dr\,(u\,dr+r\,du)+\frac{1}{r}(u\,dr+r\,du)^2\\ &=\frac{D_g}{2r}\,dr^2+r\,du^2,\qquad ds^2_g=E\,dr^2+G\,du^2=\frac{2\pi}{H}\big(D_g\,dr^2+2r^2du^2\big).\end{aligned} \tag{3.10}$$

For a real, nondegenerate outer horizon, $r>0$ and $H>0$. The coefficient of du^2 is therefore positive, and the sign of D_g decides the signature. The metric is positive definite for $D_g>0$ and indefinite for $D_g<0$. Curvature is defined on both open regions.

We use the convention $R^i{}_{jkl}=\partial_k\Gamma^i_{lj}-\partial_l\Gamma^i_{kj}+\Gamma^i_{km}\Gamma^m_{lj}-\Gamma^i_{lm}\Gamma^m_{kj}$, with $R_{jl}=R^i{}_{jil}$. In terms of E and G, the independent Christoffel symbols are given below. A subscript following a comma denotes partial differentiation.

$$\begin{aligned}&\Gamma^r_{rr}=E_{,r}/(2E),\qquad &&\Gamma^r_{ru}=E_{,u}/(2E),\qquad &&\Gamma^r_{uu}=-G_{,r}/(2E),\\ &\Gamma^u_{rr}=-E_{,u}/(2G),\qquad &&\Gamma^u_{ru}=G_{,r}/(2G),\qquad &&\Gamma^u_{uu}=G_{,u}/(2G).\end{aligned} \tag{3.11}$$

The determinant in this chart is $J=EG=8\pi^2r^2D_g/H^2$. Contracting the curvature as $R=2R_{ruru}/J$ puts the derivatives of the metric in the combination

$$R=-\frac{G_{,rr}+E_{,uu}}{J}+\frac{J_{,r}G_{,r}+J_{,u}E_{,u}}{2J^2}. \tag{3.12}$$

For this diagonal metric, differentiating at fixed u or fixed r as indicated gives

$$\begin{aligned}&G_{,r}=\frac{8\pi r(1-u^2)}{H^2},\qquad &&E_{,u}=\frac{8\pi ar^2u}{H^2},\\ &G_{,rr}=\frac{8\pi(1-u^2)(H-4ar^2)}{H^3},\qquad &&E_{,uu}=\frac{8\pi ar^2(H+4u^2)}{H^3},\\ &\frac{J_{,r}}{J}=\frac{2}{r}+\frac{2ar}{D_g}-\frac{4ar}{H},\qquad &&\frac{J_{,u}}{J}=\frac{2u}{D_g}+\frac{4u}{H}.\end{aligned} \tag{3.13}$$

With these derivatives, the scalar in Eq. (3.12) simplifies to

$$R = -\frac{a(ar^2+u^2)(ar^2+3u^2-3)}{\pi H D_g^2} = \frac{a(D_g+1)(H-2D_g)}{\pi H D_g^2}. \tag{3.14}$$

The entropy used in Eq. (31) of Ref. [19] is $\sigma = r^2$. At fixed (M, Q), our area normalization $S = \pi\sigma$ multiplies the entropy metric by π and divides its scalar curvature by π. With $a = 3/\ell^2$ the result is the first expression above. The expression on the right gives the coefficient of the pole directly. At a regular point of $D_g = 0$ with $a > 0$ and $H \neq 0$,

$$D_g^2 R\big|_{D_g=0} = \frac{a}{\pi}. \tag{3.15}$$

Since the coefficient is nonzero, the curvature has a double pole in the transverse coordinate D_g. The extremal boundary has a different local behavior. There $H = 0$ at $u^2 = 1 + ar^2$, so $D_g = 2ar^2 > 0$ for $a > 0$. Approaching from $T \neq 0$, the product HR tends to $-2a(D_g+1)/(\pi D_g) \neq 0$. The extremal pole is thus simple in the transverse coordinate H.

3.3 Heat-capacity and curvature poles in the flat and AdS families

For asymptotically flat RN ($a = 0$), the identity $D_g = -H$ holds on the entire nonextremal patch $|u| < 1$. Introducing ρ and θ in Eq. (3.10) brings the line element to the form

$$ds_g^2 = -2\pi\, dr^2 + \frac{4\pi r^2}{1-u^2}\, du^2 = -d\rho^2 + \rho^2 d\theta^2, \quad \rho = \sqrt{2\pi}\, r, \quad \theta = \sqrt{2}\arcsin u. \tag{3.16}$$

The coordinates $X = \rho\cosh\theta$ and $Y = \rho\sinh\theta$ now give $ds_g^2 = -dX^2 + dY^2$. Thus $R = 0$ follows directly from the metric, independently of Eq. (3.14), as in Ref. [19]. For $Q \neq 0$, the radius $r^2 = 3Q^2$ lies in this flat patch. There $K = -1 + 3Q^2/r^2$ has a simple zero and $H = 2/3$, so $C_{Q,P}$ has a simple pole.

With $a > 0$ and $Q \neq 0$ fixed, the locations of the heat-capacity and curvature poles follow from a pair of quadratics. Writing $x = r^2$ gives

$$xK = ax^2 - x + 3Q^2, \qquad xD_g = ax^2 - x + Q^2. \tag{3.17}$$

Their discriminants, $1 - 12aQ^2$ for K and $1 - 4aQ^2$ for D_g, place the two root mergers on different isobars. At a simple zero of K the relation $D_g = -2u^2 \neq 0$ keeps the ordinary curvature regular whenever $H \neq 0$, even as the fixed-charge heat capacity diverges.

The first merger occurs at $aQ^2 = 1/12$. Here $K = a(r^2 - r_c^2)^2/r^2$, with $r_c^2 = 1/(2a) = 6Q^2$ and $(H, D_g) = (4/3, -1/3)$ at r_c. In the factorization $r^2 - r_c^2 = (r - r_c)(r + r_c)$, the ratio $(r + r_c)/r$ tends to two. Hence K has leading term $4a(r - r_c)^2$, and

$$\lim_{r\to r_c} (r - r_c)^2 C_{Q,P} = \frac{2\pi r_c^2 (4/3)}{4a} = 48\pi Q^4, \qquad R(r_c) = \frac{3}{4\pi Q^2}. \tag{3.18}$$

A fixed-charge variation therefore encounters a double pole in the heat capacity. The full (S, Q) metric has finite scalar curvature there. Its negative determinant, signaled by $D_g = -1/3$, makes the quadratic form indefinite when entropy and charge can fluctuate together.

At the second merger, $aQ^2 = 1/4$, the square occurs in the metric determinant through $D_g = a(r^2 - r_*^2)^2/r^2$, with $r_*^2 = 1/(2a) = 2Q^2$. Along the fixed-charge path, $D_g = 4a(r - r_*)^2 + O((r - r_*)^3)$, whereas H and K both equal one at r_*. Equation (3.15) then gives

$$\lim_{r\to r_*} (r - r_*)^4 R = \frac{1}{16\pi a}, \qquad C_{Q,P}(r_*) = 2\pi r_*^2 = 4\pi Q^2. \tag{3.19}$$

The curvature has a second-order pole in the transverse coordinate D_g. Its fourth-order pole in r measures the quadratic contact of this path with $D_g = 0$. The same composition determines the pole order for higher contact. Suppose that $R = bD_g^{-2} + O(D_g^{-1})$ and that a path with parameter t satisfies $D_g(t) = c(t - t_*)^m + O((t - t_*)^{m+1})$, with $bc \neq 0$. Substitution gives $R(t) \sim bc^{-2}(t - t_*)^{-2m}$.

3.4 Thermal response at fixed electric potential

Charge can vary when the electric potential is held fixed. For a two-variable potential at fixed P, write its Hessian as $W = \left(\begin{smallmatrix} A_0 & B_0 \\ B_0 & E_0 \end{smallmatrix}\right)$. The corresponding variations satisfy $dT = A_0 dS + B_0 dQ$ and $d\Phi = B_0 dS + E_0 dQ$. If $E_0 \neq 0$, the constraint $d\Phi = 0$ sets $dQ = -B_0 dS/E_0$. Eliminating dQ from the temperature variation yields

$$\left(\frac{\partial T}{\partial S}\right)_{\Phi,P} = A_0 - \frac{B_0^2}{E_0} = \frac{\det W}{E_0}, \qquad C_{\Phi,P} = \frac{T E_0}{\det W} = \frac{2\pi r^2 H}{D_g} \quad \text{for RN–AdS.} \tag{3.20}$$

For RN–AdS, $E_0 = 1/r$ and Eq. (3.9) gives the last expression. One can also hold $u = \Phi = Q/r$ constant in the temperature formula itself, obtaining $4\pi r^2(\partial_r T)_{\Phi,P} = -1 + ar^2 + \Phi^2 = D_g$. The equation of state thus has stationary temperatures on two loci, $K = 0$ at fixed charge and $D_g = 0$ at fixed potential [22, 39, 40]. For $T > 0$, the sign of K decides local stability against entropy fluctuations at fixed Q. A simple zero of K separates the stable and unstable branches. On $D_g = 0$, the full Hessian has a null vector along which $dT = d\Phi = 0$. For $Q \neq 0$ this direction has a charge component, and the heat capacity measured with Q held fixed remains finite.

Figure 1 locates both mergers. The isobar $p = P/P_c = 1$ passes through the endpoint of small/large black-hole coexistence, where the two fixed-charge spinodals meet (Sec. 5). On the $p = 3$ isobar, D_g has a double zero and is positive immediately to either side. The contact produces the fourth-order curvature pole of Eq. (3.19). The branch retains local stability under fixed-charge variations through the point of contact.

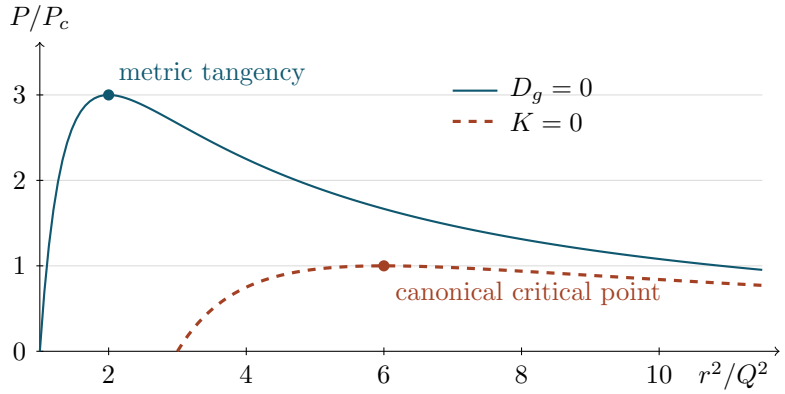

Figure 1: Fixed-potential and fixed-charge response poles for $T > 0$, in the variables $y = r^2/Q^2$ and $p = P/P_c = 12aQ^2$. On the solid curve, $p = 12(y-1)/y^2$, the full (S, Q) metric degenerates $(D_g = 0)$ and the fixed-potential heat capacity diverges. The dashed curve, $p = 12(y-3)/y^2$, follows the fixed-charge spinodal $(K = 0)$, where $C_{Q,P}$ diverges. Horizontal isobars touch the dashed curve at $(y, p) = (6, 1)$ and the solid curve at $(2, 3)$. The endpoint $(1, 0)$ of the solid curve is extremal and lies outside the $T > 0$ domain.

The neutral limit removes the mixed entropy–charge derivative, so both response poles occur at the same radius. With $a = 3/\ell^2$, the uncharged temperature $T = (1 + 3r^2/\ell^2)/(4\pi r)$ reaches its minimum at $r = \ell/\sqrt{3}$. To find the Hawking–Page transition, take thermal AdS as the free-energy reference and evaluate $G = M - TS = r(1 - r^2/\ell^2)/4$ on the black-hole branch. The free energies cross at $r = \ell$ [41], beyond the temperature minimum detected by both local responses.

4 What the optical residue determines on state space

At fixed pressure, take the charge and the independently normalized entropy as the affine variables of the enthalpy $M(S, Q)$. In this chart, Eq. (3.3) expresses the entropy metric as the Hessian of

M divided by the temperature. Since the residue gives M_S, the question is which entries of this Hessian follow by differentiation.

Proposition (reconstruction from the optical residue at fixed pressure). Consider the static family with simple horizons of Sec. 2, with the same Killing-time normalization for every member. Let the enthalpy $M(S,Q)$ and the finite, positive optical residue $b(S,Q)$ be real analytic on a coordinate rectangle $I_S \times I_Q$, with $M_S = T = (4\pi b)^{-1}$. Choose a reference entropy $S_0 \in I_S$. The entropy row of $g^R_{ij} = M_{ij}/T$ is then given by

$$g^R_{SS} = \frac{T_S}{T} = -\partial_S \log b = \frac{1}{C_{Q,P}}, \qquad g^R_{SQ} = \frac{T_Q}{T} = -\partial_Q \log b. \tag{4.1}$$

All compatible analytic enthalpies and their corresponding charge–charge metric entries satisfy

$$\begin{aligned} M(S,Q) &= \int_{S_0}^{S} T(s,Q)\, ds + F(Q), \\ T g^R_{QQ} &= \int_{S_0}^{S} \partial_Q^2 T(s,Q)\, ds + F''(Q), \end{aligned} \tag{4.2}$$

with one freely specifiable real-analytic function F on I_Q.

Proof. From $M_S = T$, the derivatives of T at fixed Q and at fixed S give M_{SS} and M_{SQ}, respectively. Dividing by T yields Eq. (4.1). Even at a zero of T_S, the reciprocal heat capacity has the regular expression T_S/T. To recover M, integrate T along a line of constant charge, starting at S_0. Its initial value is $F(Q) = M(S_0, Q)$. Two derivatives of the resulting enthalpy with respect to charge give the second line of Eq. (4.2). The difference between any two reconstructions has zero S derivative. Conversely, adding any analytic function of Q preserves M_S, which proves that the family is exhaustive. If the electric potential Φ is also known and real analytic, the rectangle admits a primitive of $T\,dS + \Phi\,dQ$ precisely when $\partial_S \Phi = \partial_Q T$. The values on the reference isentrope then give $F'(Q) = \Phi(S_0, Q)$, leaving only one additive constant in M. □

The required measurements depend on which direction one follows in state space. At a single charge, the residue as a function of entropy yields the temperature, inverse heat capacity and enthalpy differences along that line. Comparing neighboring charges at the same entropy gives the mixed derivative $\partial_S \Phi = \partial_Q T$. To obtain the charge stiffness $(\partial_Q \Phi)_{S,P} = T g^R_{QQ}$, it suffices to measure it along the isentrope $S = S_0$. Equation (4.2) fixes its dependence on entropy everywhere else in the rectangle through $\partial_S (T g^R_{QQ}) = \partial_Q^2 T$.

A common temperature field with two scalar curvatures. To see how the undetermined charge response enters the curvature, vary the coefficient of Q^2 in the following analytic potential. In dimensionless affine coordinates (S,Q), take

$$M_\lambda = \frac{S^3}{6} + SQ + \frac{\lambda Q^2}{2}, \qquad T = \frac{S^2}{2} + Q, \qquad h = M''_\lambda = \begin{pmatrix} S & 1 \\ 1 & \lambda \end{pmatrix}, \qquad \Delta = \det h = \lambda S - 1. \tag{4.3}$$

The term proportional to λ disappears on taking the entropy derivative, so every member has the same residue b and the same heat capacity $C_Q = T/S$ wherever $S \neq 0$. Restrict to a patch with $\lambda > 0$, $\Delta > 0$ and $T > 0$, where both h and h/T are positive definite. Completing the square gives $h_{ij}dx^i dx^j = \lambda(dQ + dS/\lambda)^2 + (S - 1/\lambda)dS^2$. In the coordinates $\sqrt{\lambda}(Q + S/\lambda)$ and $\int^S \sqrt{s - 1/\lambda}\, ds$, the line element is Euclidean and $R[h] = 0$. With our curvature convention, a conformal rescaling in two dimensions gives $R[h/T] = T(R[h] + \nabla_h^2 \log T)$. Since $\partial_j T = h_{Sj}$, the gradient has components $h^{ij}\partial_j \log T = \delta^i_S/T$ and only the S derivative enters its divergence. The

scalar curvature is therefore

$$R[h/T] = \frac{T}{\sqrt{\Delta}}\,\partial_S\left(\frac{\sqrt{\Delta}}{T}\right) = \frac{\partial_S\Delta}{2\Delta} - \frac{\partial_S T}{T} = \frac{\lambda}{2(\lambda S-1)} - \frac{S}{T}. \tag{4.4}$$

Evaluate the scalar at $S = Q = 1$. For $\lambda = 2$ the result is $R = 1/3$, while for $\lambda = 3$ it is $R = 1/12$. Both states have $T = 3/2$ and a positive-definite metric. These analytic potentials establish nonuniqueness within thermodynamics. Whether either enthalpy arises from a black-hole solution is a separate question.

The charge response in a fluctuation measurement. On a stable patch where entropy and charge can both fluctuate, the entropy metric gives the quadratic cost of a small fluctuation [18]. Setting $\delta Q = 0$ selects g^R_{SS}, which is the same for the two potentials. Setting $\delta S = 0$ instead selects the coefficient of $(\delta Q)^2$ in the line element, $g^R_{QQ} = (\partial_Q \Phi)_{S,P}/T$. One could distinguish the two systems by measuring the change in electric potential when a small charge is added at fixed entropy. For a given black-hole family, its electric equation of state or equivalent enthalpy data on the reference isentrope supply this information.

Recovering the temperature on a fixed-control curve. Suppose that the measured quantities are the entropy and the fixed-charge heat capacity on a connected Riemann surface parametrizing states at fixed pressure and charge. Together they define the one-form $\eta = dS/C_{Q,P}$. Wherever the temperature is finite and nonzero, the heat-capacity relation requires $\eta = dT/T = -db/b$. On a disk where η is holomorphic, a single temperature measurement $T(z_0) \neq 0$ fixes the local solution,

$$T(z) = T(z_0)\exp\left(\int_{z_0}^{z}\eta\right). \tag{4.5}$$

Now allow η to be holomorphic outside a discrete set of punctures. Changing the integration path in Eq. (4.5) multiplies the temperature by the exponential of a closed period. The temperature is therefore single valued on the punctured curve exactly when $\oint_\gamma \eta \in 2\pi i\mathbb{Z}$ for every closed path γ. Meromorphic extension across the punctures imposes one further local condition.

In a coordinate u centered at a puncture, a nonzero meromorphic temperature germ has the form $T = u^n v(u)$, with $n \in \mathbb{Z}$ and v holomorphic and nonvanishing at 0. Its logarithmic derivative $\eta = n\,du/u + dv/v$ has at most a simple pole. Conversely, suppose $\eta = (n/u + k(u))du$ with k holomorphic. The period around a small circle forces $n \in \mathbb{Z}$, and $u^n \exp(\int k\,du)$ gives the local temperature up to a nonzero constant. It extends meromorphically to $u = 0$. A pole of order $p \geq 2$ contributes a nonconstant polynomial in u^{-1} to a primitive of η. Even when the monodromy is trivial, exponentiating that polynomial gives an essential singularity. Thus entropy and heat-capacity data determine the temperature along the chosen curve up to normalization when both the period and pole conditions hold. Fixing $F(Q)$ in Eq. (4.2) requires independent information in the charge direction.

5 Fixed-charge spinodals on a complexified RN–AdS isobar

Fix the real charge $Q \neq 0$ and pressure $P = -\Lambda/(8\pi) > 0$ of a four-dimensional spherical Reissner–Nordström–AdS black hole, and take $G = \hbar = c = k_{\mathrm{B}} = 1$. The outer-horizon radius labels the equilibrium states on this isobar. We denote its complex continuation by z. Moving along the real isobar changes the mass, whereas a radial derivative of the spacetime metric holds the mass fixed. For stability at fixed charge we follow Refs. [40, 42]. Identifying P with the cosmological pressure makes M the enthalpy in the extended first law [43–45].

5.1 Temperature, optical residue, and heat capacity along the isobar

On the real isobar, the horizon equation $f(r) = 1 - 2M/r + Q^2/r^2 + 8\pi P r^2/3 = 0$ determines M as a function of r. This function and the area entropy have the continuations

$$M(z) = \frac{z}{2} + \frac{Q^2}{2z} + \frac{4\pi P}{3} z^3, \qquad S(z) = \pi z^2. \tag{5.1}$$

A prime now denotes differentiation along the isobar. The first law gives $T = M'/S'$ with $M'(z) = 1/2 - Q^2/(2z^2) + 4\pi P z^2$ and $S'(z) = 2\pi z$. Thus the temperature and its slope are

$$T(z) = \frac{1}{4\pi}\left(8\pi P z + \frac{1}{z} - \frac{Q^2}{z^3}\right) = \frac{N(z)}{4\pi z^3}, \qquad N(z) = 8\pi P z^4 + z^2 - Q^2, \tag{5.2}$$

$$T'(z) = \frac{1}{4\pi}\left(8\pi P - \frac{1}{z^2} + \frac{3Q^2}{z^4}\right) = \frac{D(z)}{4\pi z^4}, \qquad D(z) = 8\pi P z^4 - z^2 + 3Q^2. \tag{5.3}$$

One can also recover T by differentiating the lapse within a single spacetime. Holding M fixed gives $f_w = 2M/w^2 - 2Q^2/w^3 + 16\pi P w/3$. Evaluating this derivative at the horizon $w = z$ of the solution with mass $M(z)$ in Eq. (5.1) gives $f_w(z; M(z)) = N(z)/z^3 = 4\pi T(z)$. The residue is the reciprocal of this derivative. Its variation from one solution to the next follows by differentiating with respect to z,

$$b(z) = \frac{z^3}{N(z)}, \qquad b'(z) = \frac{z^2[3N(z) - zN'(z)]}{N(z)^2} = -\frac{z^2 D(z)}{N(z)^2}. \tag{5.4}$$

At nonzero temperature, b is stationary precisely at the spinodal. The charge and pressure derivatives of the enthalpy at fixed entropy give $\Phi = Q/z$ and $V = 4\pi z^3/3$, respectively, as required by $dM = T\,dS + \Phi\,dQ + V\,dP$.

Both T and T' are holomorphic for $z \neq 0$. Wherever $T' \neq 0$, we can use temperature as the local coordinate and write

$$C_{P,Q} = T\left(\frac{\partial S}{\partial T}\right)_{P,Q} = \frac{T(z)\,2\pi z}{T'(z)} = 2\pi z^2\,\frac{N(z)}{D(z)}. \tag{5.5}$$

This quotient gives the meromorphic continuation of $C_{P,Q}$. On the real outer branch with $r > 0$ and $T > 0$, its sign is the sign of D. At a positive zero of D we have $3Q^2 = r^2 - 8\pi P r^4$, so $N = (32\pi P r^4 + 2r^2)/3 > 0$ and the pole survives. For the one-form $C_{P,Q}\,dT$, the factor $dT = T'(z)\,dz$ cancels the pole,

$$C_{P,Q}\,dT = T\,dS = M'(z)\,dz. \tag{5.6}$$

Since $M'(z)$ is regular at every nonzero spinodal, the integral of $C_{P,Q}\,dT$ around a sufficiently small closed contour enclosing just that point vanishes.

5.2 Spinodal mergers and the local inverse of temperature

With $y = r^2$ the spinodal equation becomes $8\pi P y^2 - y + 3Q^2 = 0$. Its positive roots meet when the discriminant $1 - 96\pi P Q^2$ vanishes. Solving for y and evaluating Eq. (5.2) at the repeated root gives

$$y_\pm = \frac{1 \pm \sqrt{1 - 96\pi P Q^2}}{16\pi P}, \qquad P_c = \frac{1}{96\pi Q^2}, \quad r_c^2 = 6Q^2, \quad T_c = \frac{1}{3\pi r_c}. \tag{5.7}$$

The critical parameters reproduce Eqs. (3.16)–(3.18) of Ref. [45]. Fractional powers also occur in the free energy when the two Davies radii merge [46]. For $0 < P < P_c$ each positive root gives a simple zero of T'. Since D is an upward-opening quadratic in r^2, $C_{P,Q}$ is negative between the two radii. Above P_c the zeros leave the real axis, and the entire physical outer branch has

$C_{P,Q} > 0$. At P_c the factorization $D = 8\pi P_c(r^2 - r_c^2)^2$ gives a double zero. The first nonvanishing temperature derivative there is the third, as follows directly from Eq. (5.3),

$$T'' = \frac{2z^{-3} - 12Q^2 z^{-5}}{4\pi}, \qquad T''' = \frac{-6z^{-4} + 60Q^2 z^{-6}}{4\pi}, \qquad T'''(r_c) = \frac{1}{\pi r_c^4}. \tag{5.8}$$

To invert T near a zero z_0 of its derivative, set $\delta = z - z_0$ and write $T'(z) = \alpha\delta^m + O(\delta^{m+1})$ with $\alpha \neq 0$. Assume $T_0 S_0' \neq 0$, where $T_0 = T(z_0)$ and $S_0' = S'(z_0)$. Integrating T' gives the leading temperature shift, while the quotient TS'/T' gives the heat capacity,

$$T - T_0 = \frac{\alpha}{m+1}\delta^{m+1}\,[1 + O(\delta)], \qquad C_{P,Q} = \frac{T_0 S_0'}{\alpha}\,\delta^{-m}[1 + O(\delta)]. \tag{5.9}$$

The analytic factor multiplying δ^{m+1} in $T - T_0$ has no zero near $\delta = 0$. On a small disk it therefore admits a holomorphic $(m+1)$st root. Multiplying δ by that root gives a local coordinate in which $T - T_0$ is a pure $(m+1)$st power. On each branch of the inverse,

$$C_{P,Q}(T) \;\propto\; (T - T_0)^{-m/(m+1)}. \tag{5.10}$$

At an ordinary spinodal ($m = 1$), the inverse has a square-root branch point. On either adjoining real branch the heat capacity scales as $|C_{P,Q}| \propto |T - T_0|^{-1/2}$. The merger ($m = 2$) has a cube-root inverse. Along the critical isobar, $T - T_c$ is cubic to leading order in $r - r_c$, so the double pole in radius gives $|C_{P,Q}| \propto |T - T_c|^{-2/3}$. The multiplicity m survives a locally biholomorphic change of state parameter, whose Jacobian multiplies T' by a nonvanishing analytic factor. Temperature itself fails this test at a stationary point.

On the real isobar in Fig. 2, the extrema of T and b occur at the same radii and have opposite character. Since entropy increases with radius, the descending temperature branch has negative heat capacity.

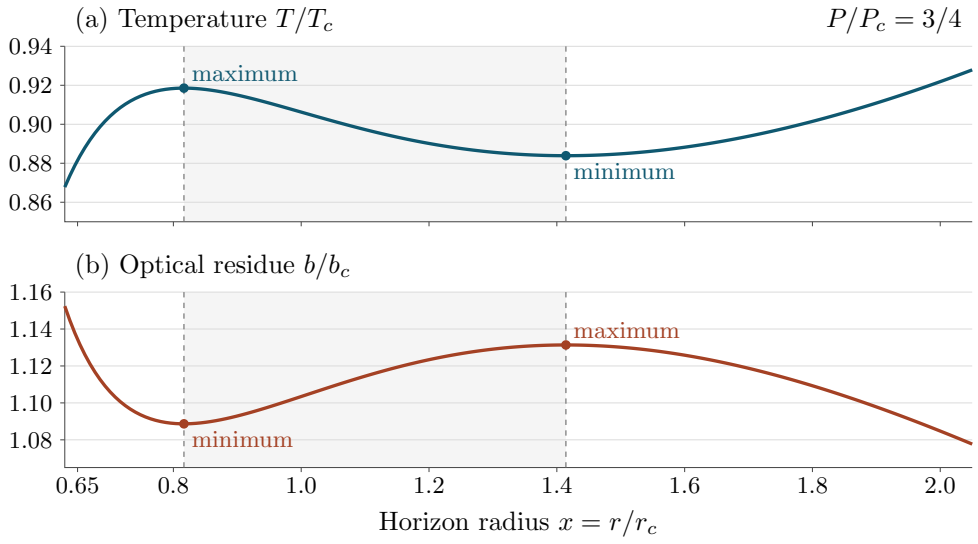

Figure 2: Reduced temperature and optical residue at $p = 3/4$. The left dashed line marks the temperature maximum at $x_- = \sqrt{2/3}$, the right one the minimum at $x_+ = \sqrt{2}$. The residue $b/b_c = T_c/T$ takes its minimum and maximum at those same radii. Shading marks the branch with $C_{P,Q} < 0$. The plotted range $0.63 \leq x \leq 2.05$ lies above the extremal radius $x_e \simeq 0.39671$ and has positive temperature throughout.

5.3 Tracking the spinodal roots across the critical pressure

Use the reduced variables $x = z/r_c$, $p = P/P_c$, and $\tau = T/T_c$. With the critical scales from Eq. (5.7), the equation of state (5.2) and its derivative become

$$\tau_p(x) = \frac{3px + 6x^{-1} - x^{-3}}{8}, \qquad \chi_p(x) = \frac{d\tau_p}{dx} = \frac{3}{8x^4}\big(px^4 - 2x^2 + 1\big). \tag{5.11}$$

Xu and Mann obtained the quartic in Eq. (5.11) from the spinodal condition [34, Eq. (8)]. We can follow its roots through the merger by integrating the logarithmic derivative of χ_p. Let Γ be a positively oriented simple closed contour on which χ_p has neither a zero nor a pole. The argument principle [47, Chap. 3] gives its winding number,

$$W_\Gamma = \frac{1}{2\pi i}\oint_\Gamma \frac{\chi_p'(x)}{\chi_p(x)}\,dx = \sum_{\text{inside }\Gamma} \operatorname{ord}_x(\chi_p). \tag{5.12}$$

Locally $\chi_p = (x - x_j)^{k_j} h_j(x)$, with $h_j(x_j) \neq 0$, so $\chi_p'/\chi_p = k_j/(x - x_j) + h_j'/h_j$ has residue k_j. Take Γ to be the circle $|x - 1| = 1/2$. It excludes the fourth-order pole at $x = 0$, whose contribution would be -4. Of the four roots specified by $x^2 = (1 \pm \sqrt{1 - p})/p$, the table gives those enclosed by Γ at three pressures.

p	Roots inside Γ	W_Γ	Distinct real roots inside Γ
$3/4$	$\sqrt{2/3},\ \sqrt{2}$	2	2
1	1 (multiplicity two)	2	1
$5/4$	$\sqrt{(4+2i)/5},\ \sqrt{(4-2i)/5}$	2	0

At $p = 5/4$ the enclosed roots have moved to approximately $0.9204 \pm 0.2173i$. No zero crosses the contour over the interval $3/4 \le p \le 5/4$. For $p \le 1$ in this interval the two positive roots lie in $[\sqrt{2/3}, \sqrt{2}]$. For $p > 1$ the roots in the right half-plane satisfy $|x^2 - 1| = \sqrt{(p-1)/p} \le 1/\sqrt{5}$. Since $|x + 1| > 1$, both have $|x - 1| < 1/2$. The other two roots remain in the left half-plane, outside the disk.

As p rises to one, the two ends of the real branch with negative heat capacity approach each other. At their meeting point the slope has a double zero. Above that pressure its zeros form a conjugate pair (Fig. 3). This motion explains how both real heat-capacity poles disappear while the contour still encloses two zeros counted with multiplicity. Only a real outer horizon with positive temperature can represent a physical spinodal. Locating coexistence requires a comparison of the free energies of two real equilibria, which we make below.

We checked the winding numerically on a circle of radius R centered at c. Sampling at $x_k = c + w_k$, where $w_k = R\exp(2\pi i k/n)$, gives the trapezoidal approximation $n^{-1}\sum_{k=0}^{n-1} w_k\,\tau_p''(x_k)/\tau_p'(x_k)$ to Eq. (5.12). Numerical differentiation of τ_p at 60 decimal digits with $n = 256$ gave an absolute error below 1.2×10^{-21} for each of the three counts. At $p = 3/4$, a circle of radius $1/12$ centered on either positive root gave index 1. At $p = 5/4$, a circle of radius $1/4$ centered at the origin gave the pole index -4.

5.4 The small- and large-black-hole coexistence radii

At fixed pressure and charge, the small and large black holes can coexist at a bath temperature T_* if each is locally stable and their Gibbs free energies agree. Equations (5.1) and (5.2) give the free energy along each equilibrium branch,

$$G(r) = M(r) - T(r)S(r) = \frac{r}{4} + \frac{3Q^2}{4r} - \frac{2\pi P}{3}r^3, \qquad dG = -S\,dT \quad (P, Q \text{ fixed}). \tag{5.13}$$

Denote the two radii by $a < b$ and write $v = ab$, $s = a + b$, and $h = a^2 + ab + b^2$. The equalities $T(a) = T(b)$ and $G(a) = G(b)$ contain a common factor $a - b$. Dividing the temperature difference

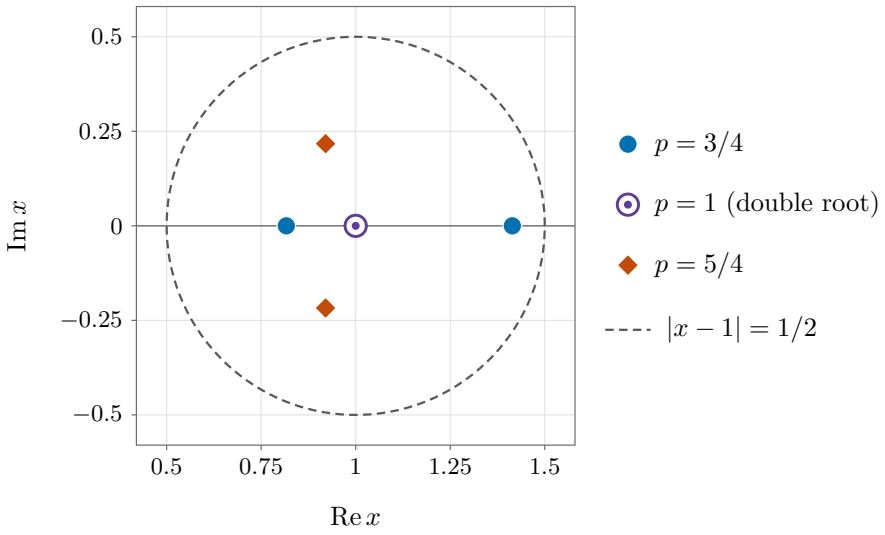

Figure 3: Motion of the zeros of $\chi_p = d(T/T_c)/dx$, with $x = z/r_c$ and $p = P/P_c$. Inside the dashed circle $|x - 1| = 1/2$, the two simple real zeros at $p = 3/4$ meet at $x = 1$ when $p = 1$. At $p = 5/4$ they occur as a conjugate pair on opposite sides of the real axis. The image of the circle under χ_p has winding number two at all three pressures.

and four times the free-energy difference by this factor gives the following pair of equations. Here the divided differences of r^{-1} and r^{-3} are $-1/v$ and $-h/v^3$, respectively.

$$8\pi P = \frac{1}{v} - \frac{Q^2 h}{v^3}, \qquad \frac{8\pi P}{3} h = 1 - \frac{3Q^2}{v}. \tag{5.14}$$

Eliminating P and multiplying through by v^3 leaves $(h - 3v)[v^2 - Q^2(h + 3v)] = 0$. The first factor equals $(a - b)^2$ and is positive for distinct states. In the second, $h + 3v = s^2 + 2v$. The product and sum of the two radii therefore satisfy

$$Q^2 = \frac{v^2}{s^2 + 2v}, \qquad 8\pi P = \frac{3Q^2}{v^2}, \qquad v = \frac{6Q^2}{\sqrt{p}}, \qquad s^2 = \frac{v^2}{Q^2} - 2v. \tag{5.15}$$

Choose the positive root for s. Since $v > 0$, the roots of $r^2 - sr + v = 0$ are both positive whenever they are real. They are distinct precisely when $s^2 - 4v = v(v/Q^2 - 6) > 0$, which restricts coexistence to $0 < p < 1$. Evaluation of the heat-capacity denominator on these roots gives

$$D(r) = \frac{2r^2(a - b)^2}{s^2 + 2v} > 0 \qquad (r = a, b). \tag{5.16}$$

At the common positive temperature, Eq. (5.16) ensures that the heat capacity is positive and finite on both branches. Their stability also follows directly from the potential $M(r) - T_* S(r)$ with the bath held at T_*. Its derivative is $[T(r) - T_*]S'(r)$. At an equilibrium radius the second derivative reduces to $T'(r)S'(r)$, so the two positive-slope branches give minima. Any intervening negative-slope branch gives a maximum. Equation (5.3) allows at most two positive turning radii of $T(r)$, and therefore at most three intersections with a given bath temperature. Appendix B.5 factors the off-shell free-energy difference to verify that both minima are global within this spherical charged family at coexistence.

At either coexistence radius, the equation of state $4\pi T = 8\pi P r + 1/r - Q^2/r^3$ yields $T_* = Q^2 s/(\pi v^2)$. For instance, at $r = a$, multiplying its right-hand side by v^3/Q^2 gives $3av + b(s^2 + 2v) - b^3 = 4vs$. Using $r_c^2 = 6Q^2$ to express T_* in units of T_c gives

$$\left(\frac{T_*}{T_c}\right)^2 = \frac{54Q^6 s^2}{v^4} = \frac{54Q^4}{v^2}\left(1 - \frac{2Q^2}{v}\right) = \frac{p}{2}(3 - \sqrt{p}). \tag{5.17}$$

The positive root reproduces the Maxwell equal-area result in Eq. (23) of Ref. [48]. For $0 < p < 1$, the two free energies cross while both phases remain locally stable. If either phase persists as a metastable state, its minimum disappears on reaching its spinodal. In the limit $p \uparrow 1$, the two radii merge at r_c and the crossing between distinct phases terminates.

5.5 Heat capacity in the normalized temperature–volume curvature

Wei, Liu and Mann construct a thermodynamic metric in the variables (T, V) [49]. For the spherical black hole, fixing $V = 4\pi r^3/3$ also fixes $S = \pi r^2$, so $C_V = 0$. To extract a curvature from this degenerate metric, they keep C_V at a small constant value during the calculation and take the limit of $R_N = C_V R_{(T,V)}$, with their sign convention. The ordinary entropy scalar in Eq. (3.14) is evaluated directly wherever the fixed-pressure metric is nondegenerate. Appendix B gives the sign conversion between the two curvature conventions. Folds in the temperature curve have been related to divergences of R_N [50].

On a given isobar let $x = r/r_c$, $\tau = T/T_c$, and $v = V/V_c = x^3$. Set $L = 3x^2 - 1$ and $B_* = 2\tau x^3$. In these variables Eq. (13) of Ref. [49] reads

$$R_N = \frac{L(L - 2B_*)}{2(L - B_*)^2} = \frac{1}{2}\left[1 - \left(\frac{B_*}{L - B_*}\right)^2\right], \tag{5.18}$$

where completing the square gives the expression on the right. The isobaric temperature derivative in Eq. (5.11) yields $L - B_* = -3(px^4 - 2x^2 + 1)/4 = -2x^4\tau_p'(x)$. Hence $B_*/(L - B_*) = -\tau/(x\tau_p')$ wherever the slope is nonzero. Since $dS/dx = 2S/x$, the heat capacity on the same isobar is $C_{P,Q} = 2S\tau/(x\tau_p')$. The curvature can therefore be written in terms of the heat capacity and entropy along the isobar,

$$R_N = \frac{1}{2}\left[1 - \left(\frac{C_{P,Q}}{2S}\right)^2\right]. \tag{5.19}$$

The equality extends meromorphically through isolated poles. At a simple spinodal with $S \neq 0$, the square in Eq. (5.19) gives R_N a double pole in r. At the canonical critical pressure $p = 1$, the heat-capacity ratio behaves as $C_{P,Q}/(2S) \sim 4Q^2/(r - r_c)^2$ by Eq. (3.18). The normalized curvature consequently behaves as $R_N \sim -8Q^4/(r - r_c)^4$. At the tangency on the $p = 3$ isobar, $C_{P,Q} = 2S$ gives $R_N = 0$, and the ordinary fixed-pressure scalar has a fourth-order pole. Both curvatures have been evaluated at the same states along the same paths. Their different singularities reflect the choice of metric and the normalization of the temperature–volume curvature.

Figure 4 shows how these limits are approached from either side of each radius. The dimensionless formulas in Appendix A give the six curves and their leading terms.

6 Discussion and conclusions

Suppose the horizon residue has been measured across an entire charged family at fixed pressure. Given the entropy coordinate, differentiating $-\log b$ with respect to S and Q recovers the entropy row of the metric. To determine the rest, one can make an electrical measurement on a single reference isentrope. The potential $\Phi(S_0, Q)$ fixes the derivative of $F(Q) = M(S_0, Q)$, leaving only an additive constant in the enthalpy. Without that measurement, even two positive-definite metrics can assign different curvatures to the same temperature field. This reasoning also presumes that the thermodynamic mass has been identified. With unconventional spacetime asymptotics, that identification can remain open even when the optical residue is well defined [13].

The RN–AdS equation of state lets us identify the fluctuation associated with each pole. At fixed pressure, the slope taken at fixed charge gives $K = 4\pi r^2(\partial_r T)_{Q,P}$. Holding the electric potential fixed gives $D_g = 4\pi r^2(\partial_r T)_{\Phi,P}$. The ordinary (S, Q) metric becomes degenerate at $D_g = 0$. Near a regular point of this locus $D_g^2 R \to 8P$, so quadratic contact along the fixed-charge

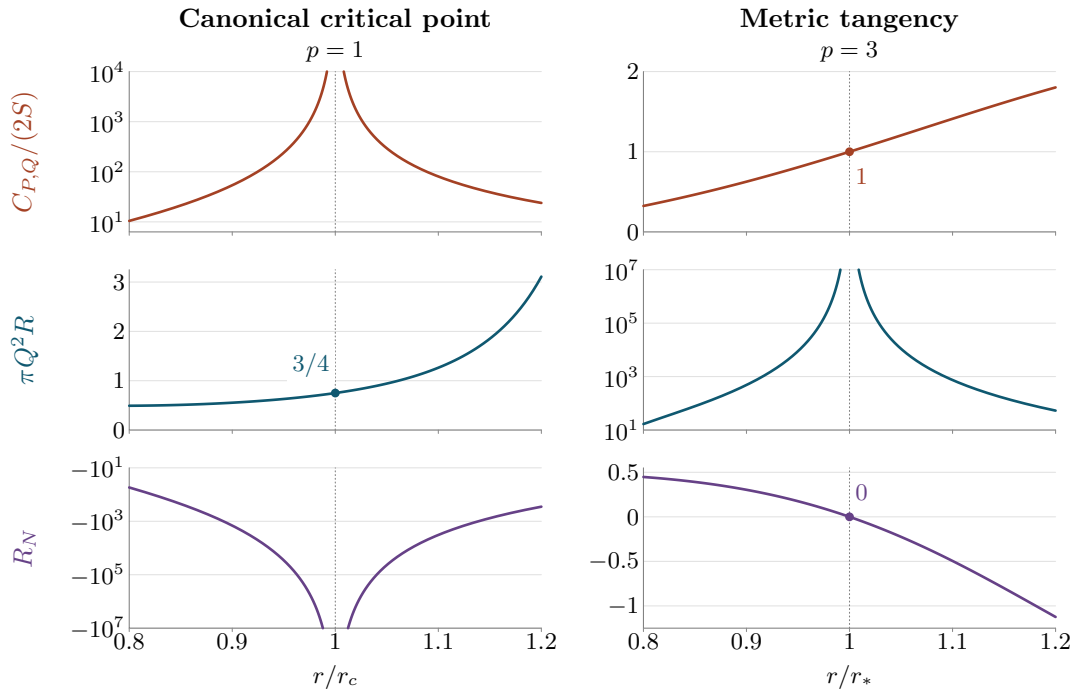

Figure 4: Heat capacity and curvature along two fixed-charge isobars. The left column passes through the canonical critical point at $p = 1$, $r_c^2 = 6Q^2$. The right column passes through the tangency to the metric-degeneracy locus at $p = 3$, $r_*^2 = 2Q^2$. The rows give the heat-capacity ratio $C_{P,Q}/(2S)$, the scaled scalar $\pi Q^2 R$ of the fixed-pressure (S, Q) metric, and the normalized (T, V) curvature R_N from Eq. (5.19). At r_c, $K = 0$ produces divergences in the first and third rows, and $D_g = -1/3$ leaves the middle row finite. At r_*, $D_g = 0$ produces a pole in the middle row, and the other two rows reach 1 and 0, respectively. Dotted lines locate r_c and r_*. Filled circles mark finite values. The divergent panels show magnitude on a logarithmic scale with signed tick labels and clip the curves at the frame. The finite panels have linear scales.

isobar at $3P_c$ produces a fourth-order pole in r. At the canonical critical point the same scalar is finite, $R = 3/(4\pi Q^2)$. The normalized (T, V) curvature R_N diverges there because Eq. (5.19) ties it to the fixed-charge heat capacity [49,50]. The partially transformed potential in (S, Φ) [51] and the canonical free-energy metric [52] likewise correspond to specific choices of fluctuations. A comparison of pole orders therefore has to specify both the metric and the path to the singular state.

The physical meaning of a contour count depends on the function being continued. At a prescribed bath temperature, real outer horizons satisfying the temperature-matching equation give candidate equilibria [30]. A signed index can also be assigned on the real axis to a zero of the inverse heat capacity [53], and Lee–Yang zeros refer to a statistical partition function [54]. Here we continue the *derivative* of the horizon temperature. On the contour of Fig. 3, its index stays at two over the pressure interval shown, even after both roots have left the physical branch. For a subcritical isobar, the coexistence temperature is selected by the crossing of the Gibbs free energies at two distinct real radii. Each phase still has a finite heat capacity at that crossing.

Reproducibility. The LaTeX source contains the four vector figures. Appendix A gives the functions needed to reproduce the six curves in Fig. 4, including their finite limits and leading pole coefficients. Appendix B supplies the intermediate algebra for the horizon, metric, spinodal and coexistence calculations. The numerical winding counts can be repeated using the contour, quadrature rule and working precision specified in Sec. 5.

A Dimensionless curves on the two limiting isobars

Figure 4 uses $t = r/r_0$ so that the radius of interest falls at $t = 1$ in both columns. The left column uses $r_0 = r_c$ and the right uses $r_0 = r_*$. Defining $j = r_0^2/Q^2$ gives $(p, j) = (1, 6)$ on the critical isobar and $(p, j) = (3, 2)$ on the tangent isobar. Since $ar_0^2 = 1/2$ in both cases, Eq. (3.7) reduces to

$$H = 1 + \frac{t^2}{2} - \frac{1}{jt^2}, \qquad D_g = -1 + \frac{t^2}{2} + \frac{1}{jt^2}, \qquad K = -1 + \frac{t^2}{2} + \frac{3}{jt^2}. \tag{A.1}$$

Inserting these expressions into Eqs. (3.9), (3.14), and (5.19) gives the ordinates of the three rows,

$$\frac{C_{P,Q}}{2S} = \frac{H}{K}, \qquad \pi Q^2 R = \frac{p}{12}\frac{(D_g + 1)(H - 2D_g)}{HD_g^2}, \qquad R_N = \frac{1}{2}\left[1 - \left(\frac{H}{K}\right)^2\right]. \tag{A.2}$$

Evaluating these functions for $0.8 \le t \le 1.2$, away from their poles, reproduces the curves. Their behavior at the marked radii follows by expanding in $\epsilon = t - 1$.

On the critical isobar ($p = 1$), $K = (t^2 - 1)^2/(2t^2) = 2\epsilon^2 + O(\epsilon^3)$, while $H = 4/3$ and $D_g = -1/3$ at $t = 1$. The leading terms in the heat-capacity ratio and the normalized curvature are therefore $2/(3\epsilon^2)$ and $-2/(9\epsilon^4)$, respectively. The ordinary curvature has the finite limit $\pi Q^2 R \to 3/4$.

On the tangent isobar ($p = 3$), the double zero belongs to $D_g = (t^2 - 1)^2/(2t^2)$. With $H = K = 1$ at the contact, the ordinary curvature satisfies $\pi Q^2 R \sim 1/(16\epsilon^4)$. The ratio $C_{P,Q}/(2S)$ tends to one there, and the normalized curvature R_N tends to zero.

B Detailed derivations

Both subscript orders $C_{Q,P}$ and $C_{P,Q}$ denote the heat capacity at fixed charge and pressure. The calculations below use the curvature convention of Sec. 3.2 for the entropy metric. The last subsection converts explicitly to the convention used for the normalized temperature–volume curvature. Throughout the RN–AdS calculation, pressure and charge are real and fixed unless a partial derivative specifies a different constraint.

B.1 The optical pole, Euclidean regularity and the first law

From a metric zero to an optical pole. Set $\xi = w - h$ and shrink the disk around h until both A/ξ and B/ξ are holomorphic and nonvanishing. In the notation of Sec. 2, put $c = a_2/a_1 + b_2/b_1$. Multiplication of the two Taylor series gives

$$\begin{aligned} AB &= a_1 b_1 \xi^2 + (a_1 b_2 + a_2 b_1)\xi^3 + O(\xi^4) = a_1 b_1 \xi^2 \big[1 + c\xi + O(\xi^2)\big], \\ (AB)^{1/2} &= \sqrt{a_1 b_1}\, \xi \big[1 + c\xi/2 + O(\xi^2)\big], \\ \omega = (AB)^{-1/2} d\xi &= \frac{1}{\sqrt{a_1 b_1}} \big[\xi^{-1} - c/2 + O(\xi)\big] d\xi. \end{aligned}$$

The middle line uses the branch fixed by $\xi > 0$. Only $\xi^{-1} d\xi$ integrates to $2\pi i$ on a positive circle. Hence $b = (a_1 b_1)^{-1/2}$ and a primitive changes by $2\pi i b$. In comparison, writing $A = \xi A_0(\xi)$ gives $dA/A = d\xi/\xi + dA_0/A_0$, whose second term is holomorphic.

Euclidean period and the outer boundary. After $t = -i\tau$, the radial and time coefficients at $\xi = b_1 \rho^2/4$ obey

$$\begin{aligned} B &= (b_1^2 \rho^2/4)[1 + O(\rho^2)], & \frac{(d\xi/d\rho)^2}{B} &= \frac{b_1^2 \rho^2/4}{(b_1^2 \rho^2/4)[1 + O(\rho^2)]} = 1 + O(\rho^2), \\ A &= (a_1 b_1/4)\rho^2 [1 + O(\rho^2)], & \frac{\beta\sqrt{A}}{\int_0^\rho \sqrt{g_{\rho\rho}}\, d\rho'} &\longrightarrow \frac{\beta\sqrt{a_1 b_1}}{2}. \end{aligned}$$

The circumference divided by the proper radius tends to 2π at a regular origin. Thus $\beta = 4\pi b$ and $T_H = \beta^{-1} = \kappa/(2\pi)$ with $\kappa = \sqrt{a_1 b_1}/2$.

To check the orientation in the disk calculation, let $A = B = f$ with $f > 0$ for $h < w \le L$ and use the smooth period at h. The orbit-space metric and its inverse have diagonal entries $(f, 1/f)$ and $(1/f, f)$ in the order (τ, w). The connection formula gives $\Gamma^w_{\tau\tau} = -ff'/2$, $\Gamma^\tau_{\tau w} = f'/(2f)$, and $\Gamma^w_{ww} = -f'/(2f)$. Since $\det g = 1$, the trace Γ^i_{iw} vanishes. The two diagonal Ricci components in the curvature convention of the text reduce to

$$\begin{aligned} R_{\tau\tau} &= \partial_w(-ff'/2) - 2\big(f'/(2f)\big)(-ff'/2) = -ff''/2, \\ R_{ww} &= \partial_w\big(-f'/(2f)\big) - \big(f'/(2f)\big)^2 - \big(-f'/(2f)\big)^2 = -f''/(2f). \end{aligned}$$

Contraction yields $R^{(2)} = R_{\tau\tau}/f + f R_{ww} = -f''$. On the outer circle, a unit tangent is $e = f^{-1/2}\partial_\tau$ and the inward unit normal is $n = -\sqrt{f}\,\partial_w$. Here $\nabla_e e = -f'\partial_w/2$, so the signed geodesic curvature is $g(\nabla_e e, n) = f'/(2\sqrt{f})$. Multiplication by $ds = \sqrt{f}\, d\tau$ gives the signed boundary term $f'(L)d\tau/2$ at $w = L$. With Gaussian curvature $R^{(2)}/2$, Gauss–Bonnet reads

$$2\pi = \frac{\beta}{2}\big[f'(h) - f'(L)\big] + \frac{\beta}{2} f'(L) = \frac{\beta f'(h)}{2}.$$

Thus $\beta = 4\pi/f'(h)$, as follows also from $b = 1/f'(h)$.

Variation across solutions. For the factorization in Eq. (2.7), Cauchy's formula on a circle that contains only $h(z)$ evaluates the integral as $b(z) = U(h(z), z)^{-1}$. Taking the ordinary derivative gives $b' = -U^{-2}(U_w h' + U_z)$, with all factors evaluated at $(h(z), z)$. For a radial change $w - h = jv + O(v^2)$ with $j \neq 0$, one has $dw/(w - h) = (v^{-1} + O(1))dv$. The residue therefore survives the change of radius. For a future-directed change of time $\tilde{t} = \lambda t$, $\lambda > 0$, the new metric coefficient is $\tilde{A} = A/\lambda^2$. Thus $\tilde{b} = \lambda b$ and $d\log\tilde{b} = d\log b + d\log\lambda$. The second term vanishes for a common rescaling.

At fixed work variables, $dM = T\, dS$ and $T = (4\pi b)^{-1}$ give $S' = M'/T = 4\pi b M'$. Integration yields the entropy difference in Eq. (2.8). For $S' \neq 0$, differentiation of the temperature and

evaluation of $C = T(\partial S/\partial T)$ give

$$T' = -\frac{b'}{4\pi b^2}, \qquad C^{-1} = \frac{T'}{TS'} = -\frac{b'}{bS'}, \qquad C = -\frac{bS'}{b'} \quad (b' \neq 0).$$

When Q and P vary, the first law replaces dM/T by $\alpha = (dM - \Phi\, dQ - V\, dP)/T$. The integral of α defines an entropy difference locally if $d\alpha = 0$. Two integration paths with the same endpoints differ by a closed loop, so path independence on the entire patch requires all periods of α to vanish. For Schwarzschild, $1/f = w/(w-2M) = 1 + 2M/(w-2M)$. With $z = 2M$, one gets $b = z$, $T = (4\pi z)^{-1}$, $M' = 1/2$, and $S' = 2\pi z$. These give $C = -2\pi z^2 = -8\pi M^2$.

Extremal RN. Write $\Delta = r_+ - r_- > 0$, with $0 < |Q| < M$. For $\omega = w^2 dw/[(w-r_+)(w-r_-)]$, multiplication by $w - r_\pm$ and evaluation at the corresponding root gives $b_+ = r_+^2/\Delta$ and $b_- = -r_-^2/\Delta$. Their sum is $(r_+^2 - r_-^2)/\Delta = r_+ + r_-$. As both radii tend to $r_e = |Q| > 0$, the outer temperature $\Delta/(4\pi r_+^2)$ tends to zero. At coalescence write $w = r_e + \xi$ to obtain $w^2/(w-r_e)^2 = r_e^2/\xi^2 + 2r_e/\xi + 1$. The coefficient $2r_e$ agrees with the sum of the two residues. On the exterior of the extremal solution, $d\ell = dw/\sqrt{f} = (1 + r_e/\xi)d\xi$, and integration from ϵ to a fixed $\xi_0 > 0$ gives $\xi_0 - \epsilon + r_e \log(\xi_0/\epsilon) \to \infty$. There is no finite-distance origin at which a conical regularity condition could select a period.

B.2 From the fundamental relation to the curvature scalar

At fixed pressure write $A_0 = M_{SS}$, $B_0 = M_{SQ}$, and $E_0 = M_{QQ}$. The inverse first law $dS = (dM - \Phi\, dQ)/T$ gives the derivative operators in the entropy representation,

$$\partial_M|_Q = T^{-1}\, \partial_S|_Q\,, \qquad \partial_Q|_M = \partial_Q|_S - \frac{\Phi}{T}\, \partial_S|_Q\,.$$

Apply them to $S_M = 1/T$ and $S_Q|_M = -\Phi/T$, using $T_S = A_0$, $T_Q = \Phi_S = B_0$, and $\Phi_Q = E_0$ on the right. This gives all three independent entries of the entropy Hessian in (M, Q),

$$\begin{aligned} S_{MM} &= -A_0/T^3, \\ S_{MQ} &= -B_0/T^2 + \Phi A_0/T^3, \\ S_{QQ}|_M &= -E_0/T + 2\Phi B_0/T^2 - \Phi^2 A_0/T^3. \end{aligned}$$

The quadratic form of the negative Hessian thus groups as

$$\frac{A_0}{T^3}(dM - \Phi\, dQ)^2 + \frac{2B_0}{T^2}(dM - \Phi\, dQ)dQ + \frac{E_0}{T}\, dQ^2.$$

Putting $dM - \Phi\, dQ = T\, dS$ gives Eq. (3.3), including the single factor $1/T$ common to all entries.

For RN–AdS, $M_r = (1 + ar^2 - Q^2/r^2)/2$, $M_Q = Q/r$ and $S_r = 2\pi r$. Hence

$$T = \frac{M_r}{S_r} = \frac{r^{-1} + ar - Q^2 r^{-3}}{4\pi}, \quad A_0 = \frac{-r^{-2} + a + 3Q^2 r^{-4}}{8\pi^2 r}, \quad B_0 = -\frac{Q}{2\pi r^3}, \quad E_0 = \frac{1}{r}.$$

Taking the determinant gives

$$A_0 E_0 - B_0^2 = \frac{-1 + ar^2 + 3Q^2/r^2 - 2Q^2/r^2}{8\pi^2 r^4} = \frac{D_g}{8\pi^2 r^4}.$$

To diagonalize the numerator W of $g = W/T$, insert $dS = 2\pi r\, dr$ and $dQ = u\, dr + r\, du$. Its mixed coefficient is $-2u + 2u = 0$, its dr^2 coefficient is $K/(2r) - 2u^2/r + u^2/r = D_g/(2r)$, and its du^2 coefficient is r. Division by $T = H/(4\pi r)$ yields $E = 2\pi D_g/H$, $G = 4\pi r^2/H$, and $J = EG = 8\pi^2 r^2 D_g/H^2$.

For a diagonal metric the convention of Sec. 3.2 gives $R_{ruru} = E R^r{}_{uru}$. The derivative terms are $E[\partial_r(-G_r/(2E)) - \partial_u(E_u/(2E))]$. The four connection products, including their signs and

the factor E, are $-E_rG_r/(4E)$, $E_uG_u/(4G)$, $-E_u^2/(4E)$, and $G_r^2/(4G)$. Expanding the two derivatives and collecting gives

$$\begin{aligned} 2R_{ruru} &= -(G_{rr}+E_{uu}) + \frac{G_r}{2}\left(\frac{E_r}{E}+\frac{G_r}{G}\right) + \frac{E_u}{2}\left(\frac{E_u}{E}+\frac{G_u}{G}\right) \\ &= -(G_{rr}+E_{uu}) + \frac{G_rJ_r+E_uJ_u}{2J}. \end{aligned}$$

Contraction gives $R = 2R_{ruru}/J$. This formula is rational and therefore also applies on the indefinite real patch $J<0$.

For the remaining algebra put $m=ar^2$, $n=u^2$, so $H=1+m-n$ and $D_g=-1+m+n$. In this calculation r and u are independent coordinates. At fixed u, $H_r=(D_g)_r=2ar$. At fixed r, $H_u=-2u$ and $(D_g)_u=2u$. Consequently

$$\begin{aligned} G_r &= 4\pi(2rH-2ar^3)/H^2 = 8\pi r(1-n)/H^2, \\ E_u &= 2\pi(2uH+2uD_g)/H^2 = 8\pi mu/H^2, \\ G_{rr}+E_{uu} &= \frac{8\pi}{H^3}\big[(1-n)(H-4m)+m(H+4n)\big], \\ \frac{J_r}{J} &= \frac{2}{r}+\frac{2ar}{D_g}-\frac{4ar}{H}, \qquad \frac{J_u}{J} = \frac{2u}{D_g}+\frac{4u}{H}. \end{aligned}$$

Substituting in JR and factoring out $8\pi/H^3$ leaves

$$\begin{aligned} \frac{JH^3R}{8\pi} =& -(1-n)(H-4m)-m(H+4n) \\ &+H(1-n)\left(1+\frac{m}{D_g}-\frac{2m}{H}\right)+Hmn\left(\frac{1}{D_g}+\frac{2}{H}\right) \\ =& \, m\left(2-4n-H+\frac{H}{D_g}\right). \end{aligned}$$

The remaining numerator obeys

$$(2-4n-H)D_g+H = (1-m-3n)D_g+H = (m+n)(3-m-3n) = (D_g+1)(H-2D_g).$$

Restoring J and $m=ar^2$ gives $R=a(D_g+1)(H-2D_g)/(\pi HD_g^2)$. Thus $D_g^2R\to a/\pi$ at $D_g=0$ with $H\neq 0$. At $H=0$ one has $D_g=2ar^2$, so $HR\to -2a(D_g+1)/(\pi D_g)$ for $a>0$. Setting $a=0$ at a nonextremal state instead gives $D_g=-H$ and $R=0$.

Finally, the two heat capacities compare different derivatives of the same temperature. At fixed Q,

$$4\pi T_r = -r^{-2}+a+3Q^2r^{-4} = \frac{K}{r^2}.$$

At fixed $\Phi=u$, differentiation of $4\pi T=(1-u^2)/r+ar$ gives $4\pi T_r=D_g/r^2$. Since $S_r=2\pi r$, the ratios TS_r/T_r are $2\pi r^2H/K$ and $2\pi r^2H/D_g$, respectively. Equivalently, fixing Φ imposes $dQ=-B_0\,dS/E_0$, whence $dT=(A_0-B_0^2/E_0)dS=(\det W/E_0)dS$. When $Q=0$ both denominators reduce to $-1+ar^2$. The mass and temperature give $M-TS=r/2+ar^3/6-r(1+ar^2)/4=r(1-ar^2/3)/4$. For $a=3/\ell^2>0$, its positive zero is ℓ, whereas the common heat-capacity pole is at $1/\sqrt{a}=\ell/\sqrt{3}$.

B.3 Reconstruction, the charge derivative, and the curvature example

Integration on a real state rectangle. Hold P fixed and take $T=(4\pi b)^{-1}$. For $i=S,Q$, the reciprocal rule gives

$$\partial_iT = -\frac{\partial_ib}{4\pi b^2}, \qquad \frac{\partial_iT}{T} = -\frac{\partial_ib}{b} = -\partial_i\log b.$$

At fixed charge, $dT = T_S\,dS$, hence $C_{Q,P} = T/T_S$ wherever $T_S \neq 0$. Its reciprocal extends as T_S/T to $T_S = 0$. Differentiating $M_S = T$ at fixed Q gives $g^R_{SS} = T_S/T$, and differentiating it at fixed S gives $g^R_{SQ} = T_Q/T$.

Set $F(Q) = M(S_0, Q)$. At each charge, the fundamental theorem of calculus gives the first line below. Since both entropy endpoints are fixed when differentiating in Q, the next two lines follow by differentiation under the integral sign.

$$\begin{aligned} M(S,Q) &= F(Q) + \int_{S_0}^{S} T(s,Q)\,ds, \\ \Phi(S,Q) = M_Q(S,Q) &= F'(Q) + \int_{S_0}^{S} T_Q(s,Q)\,ds, \\ Tg^R_{QQ} = M_{QQ}(S,Q) &= F''(Q) + \int_{S_0}^{S} T_{QQ}(s,Q)\,ds. \end{aligned}$$

In particular, the change of Tg^R_{QQ} along any line of constant charge is fixed by T_{QQ}. Two compatible enthalpies differ by a function H satisfying $H_S = 0$ throughout the rectangle. Integrating at fixed Q gives $H(S,Q) = H(S_0,Q)$, so this exhausts the freedom in the choice of F.

If Φ is supplied independently, a twice differentiable primitive requires $\Phi_S = M_{QS} = M_{SQ} = T_Q$. To verify sufficiency, choose $Q_0 \in I_Q$ and $M_0 = M(S_0, Q_0)$. First integrate along the reference isentrope and then along the fixed-charge line. The resulting candidate and its derivatives are

$$\begin{aligned} M(S,Q) &= M_0 + \int_{Q_0}^{Q} \Phi(S_0,q)\,dq + \int_{S_0}^{S} T(s,Q)\,ds, \\ M_S(S,Q) &= T(S,Q), \\ M_Q(S,Q) &= \Phi(S_0,Q) + \int_{S_0}^{S} T_Q(s,Q)\,ds \\ &= \Phi(S_0,Q) + \int_{S_0}^{S} \partial_s \Phi(s,Q)\,ds = \Phi(S,Q). \end{aligned}$$

Consequently M_0 is the only free constant once T and a compatible Φ have been prescribed. In particular, $\Phi(S_0,Q)$ alone fixes $F'(Q)$ for the reconstruction.

Curvature of the common-temperature example. For $M_\lambda = S^3/6 + SQ + \lambda Q^2/2$, two differentiations give

$$\begin{aligned} &M_S = S^2/2 + Q = T, && M_Q = S + \lambda Q, && \\ &h_{SS} = S, && h_{SQ} = 1, && h_{QQ} = \lambda, \\ &\Delta = S\lambda - 1, && h^{-1} = \Delta^{-1} \begin{pmatrix} \lambda & -1 \\ -1 & S \end{pmatrix}. && \end{aligned}$$

When $\lambda > 0$ and $\Delta > 0$, $S > 1/\lambda > 0$. The two leading principal minors of h are then positive, and $g^R = h/T$ is positive definite wherever $T > 0$. To compute the curvature, first complete the square and set

$$\begin{aligned} h_{ij}\,dx^i dx^j &= \lambda(dQ + dS/\lambda)^2 + (S - 1/\lambda)\,dS^2, \\ X = \sqrt{\lambda}(Q + S/\lambda), &\qquad Y = \tfrac{2}{3}(S - 1/\lambda)^{3/2}. \end{aligned}$$

Here $dX = \sqrt{\lambda}(dQ + dS/\lambda)$ and $dY = \sqrt{S - 1/\lambda}\,dS$, so $h = dX^2 + dY^2$. In these coordinates $g^R = e^{2\sigma} h$ with $\sigma = -\frac{1}{2}\log T$. To track the curvature sign, let i, j, k run over X, Y and write $\sigma_i = \partial_i \sigma$ and $\sigma^i = \delta^{ij}\sigma_j$. Substitution of $g^R_{ij} = e^{2\sigma}\delta_{ij}$ into the Christoffel formula gives

$$\Gamma^i{}_{jk} = \delta^i_j \sigma_k + \delta^i_k \sigma_j - \delta_{jk}\sigma^i.$$

In the Ricci convention of Sec. 3, the derivative terms are

$$\partial_k \Gamma^k{}_{ij} = 2\partial_i\partial_j\sigma - \delta_{ij}(\partial_X^2 + \partial_Y^2)\sigma,$$
$$\partial_j \Gamma^k{}_{ki} = 2\partial_i\partial_j\sigma.$$

The products $\Gamma^k{}_{km}\Gamma^m{}_{ij}$ and $\Gamma^k{}_{jm}\Gamma^m{}_{ki}$ both equal $4\sigma_i\sigma_j - 2\delta_{ij}\delta^{kl}\sigma_k\sigma_l$ in two dimensions and cancel in R_{ij}. Contracting the remaining term with $e^{-2\sigma}\delta^{ij}$ gives

$$R[g^R] = -2e^{-2\sigma}(\partial_X^2 + \partial_Y^2)\sigma = T\nabla_h^2 \log T.$$

To evaluate this scalar Laplacian, return to (S, Q). The column vector of first derivatives of T is $(S, 1)^{\mathsf{T}}$. Hence

$$h^{-1}\begin{pmatrix}\partial_S \log T \\ \partial_Q \log T\end{pmatrix} = \frac{1}{T\Delta}\begin{pmatrix}\lambda & -1 \\ -1 & S\end{pmatrix}\begin{pmatrix}S \\ 1\end{pmatrix} = \begin{pmatrix}1/T \\ 0\end{pmatrix},$$
$$R[g^R] = \frac{T}{\sqrt{\Delta}}\,\partial_S\left(\frac{\sqrt{\Delta}}{T}\right)$$
$$= \frac{T}{\sqrt{\Delta}}\left(\frac{\partial_S\Delta}{2\sqrt{\Delta}\,T} - \frac{\sqrt{\Delta}\,\partial_S T}{T^2}\right) = \frac{\lambda}{2(\lambda S - 1)} - \frac{S}{T}.$$

At $S = Q = 1$, $T = 3/2$, $C_Q = T/S = 3/2$, and

$$g_\lambda^R = \tfrac{2}{3}\begin{pmatrix}1 & 1 \\ 1 & \lambda\end{pmatrix}, \qquad \det g_\lambda^R = \tfrac{4}{9}(\lambda - 1),$$
$$R[g_2^R] = \frac{2}{2(2-1)} - \frac{2}{3} = \frac{1}{3}, \qquad R[g_3^R] = \frac{3}{2(3-1)} - \frac{2}{3} = \frac{1}{12}.$$

The positive entry $g_{SS}^R = 2/3$ and positive determinants $4/9$ and $8/9$ verify stability of both quadratic forms at the test point. Their charge entries are $4/3$ and 2, respectively.

Periods and extension on a complex state curve. On a regular fixed-P, Q arc with local coordinate z, divide $C_{Q,P} = TS'(z)/T'(z)$ into $dS = S'(z)\,dz$. This gives $\eta = T'(z)\,dz/T(z)$. The equality continues across removable zeros by analytic continuation. Integrating from a point z_0 with a measured $T_0 \neq 0$ gives $T(z) = T_0 \exp(\int_{z_0}^z \eta)$. If γ_1 and γ_2 are two paths with these endpoints, their temperatures obey

$$\frac{T_{\gamma_1}(z)}{T_{\gamma_2}(z)} = \exp\left(\int_{\gamma_1}\eta - \int_{\gamma_2}\eta\right) = \exp\left(\oint_{\gamma_1\gamma_2^{-1}}\eta\right).$$

This ratio equals one for every such pair precisely when every period lies in $2\pi i\mathbb{Z}$. Any two globally defined nonzero solutions then have constant ratio, since $d(T_1/T_2) = (T_1/T_2)(dT_1/T_1 - dT_2/T_2) = 0$. The measurement fixes this constant.

For a puncture at $u = 0$ with a meromorphic differential, write the Laurent expansion as

$$\eta = \left(\sum_{j=2}^{p} a_{-j}u^{-j} + \frac{a_{-1}}{u} + k(u)\right)du,$$

where k is holomorphic. The sum is empty at a simple pole or a regular point. Choose a local primitive $K' = k$. Integration and exponentiation on a slit disk give, for a nonzero constant A,

$$\int \eta = \sum_{j=2}^{p}\frac{a_{-j}}{1-j}u^{1-j} + a_{-1}\log u + K(u) + \text{constant},$$
$$T(u) = A\,u^{a_{-1}}e^{K(u)}\exp\left(\sum_{j=2}^{p}\frac{a_{-j}}{1-j}u^{1-j}\right).$$

One turn around the puncture multiplies T by $e^{2\pi i a_{-1}}$. Thus $a_{-1} = n \in \mathbb{Z}$ is required for single valuedness. If the sum is empty, $Ae^{K(u)}$ is a holomorphic unit. The factor u^n then gives a zero for $n > 0$, a pole for $n < 0$, and a regular nonzero value for $n = 0$. Conversely, every nonzero meromorphic germ has the form $u^n v(u)$ with $v(0) \neq 0$ holomorphic. Differentiating gives $dT/T = n\,du/u + dv/v$, which has at most a simple pole. Thus if $p \geq 2$ and $a_{-p} \neq 0$, a single-valued solution has an isolated essential singularity even when all periods satisfy the integrality condition.

B.4 From the horizon equation to the spinodal index

Temperature and heat capacity. Start at fixed $P > 0$ and $Q \neq 0$. Multiplying the horizon equation $f(z) = 0$ by z gives

$$2M = z + \frac{Q^2}{z} + \frac{8\pi P}{3} z^3, \qquad M' = \frac{1}{2} - \frac{Q^2}{2z^2} + 4\pi P z^2, \qquad S' = 2\pi z.$$

Taking their quotient gives T. Differentiating this quotient gives the slope,

$$T = \frac{M'}{S'} = \frac{1 + 8\pi P z^2 - Q^2/z^2}{4\pi z} = \frac{N}{4\pi z^3}, \qquad T' = \frac{zN' - 3N}{4\pi z^4}.$$

Using $N = 8\pi P z^4 + z^2 - Q^2$ gives $zN' - 3N = (32\pi P z^4 + 2z^2) - (24\pi P z^4 + 3z^2 - 3Q^2) = D$. For an independent temperature calculation, differentiate the lapse in w at fixed mass. Inserting the horizon mass only after this differentiation gives

$$f_w|_{w=z} = \frac{2M}{z^2} - \frac{2Q^2}{z^3} + \frac{16\pi P z}{3} = \frac{1}{z} + \frac{Q^2}{z^3} + \frac{8\pi P z}{3} - \frac{2Q^2}{z^3} + \frac{16\pi P z}{3} = \frac{N}{z^3}.$$

Hence $b = z^3/N$, and $b' = z^2(3N - zN')/N^2 = -z^2 D/N^2$. At fixed S the radius is fixed on the chosen branch. The derivatives of the horizon mass are then $M_Q = Q/z$ and $M_P = 4\pi z^3/3$. Along the isobar these same functions give

$$C_{P,Q} = \frac{N}{4\pi z^3}(2\pi z)\frac{4\pi z^4}{D} = 2\pi z^2 \frac{N}{D}, \qquad C_{P,Q} T' = \frac{N}{2z^2} = M'.$$

There is no common root of N and D in the complex z-plane for these real controls. Indeed $N - D = 2(z^2 - 2Q^2)$, and at $z^2 = 2Q^2$ both polynomials equal $Q^2(1 + 32\pi P Q^2) > 0$. Every zero of D is thus a pole of the heat capacity, with the same multiplicity. Multiplying by dT cancels it exactly, as in Eq. (5.6).

Critical radius and branch exponents. Writing $y = z^2$ in $D = 0$ gives $8\pi P y^2 - y + 3Q^2 = 0$. Its discriminant is $1 - 96\pi P Q^2$, and the quadratic formula gives $y_\pm = (1 \pm \sqrt{1 - 96\pi P Q^2})/(16\pi P)$. At the double root,

$$P_c = \frac{1}{96\pi Q^2}, \qquad r_c^2 = \frac{1}{16\pi P_c} = 6Q^2, \qquad T_c = \frac{1 + 1/2 - 1/6}{4\pi r_c} = \frac{1}{3\pi r_c}.$$

On the positive-temperature branch $N > 0$. Thus below P_c the heat capacity is negative between the two simple positive radii, where $D < 0$. Above P_c the quadratic has no real root and $D > 0$. At P_c it factors as $D = 8\pi P_c (z^2 - r_c^2)^2$. Differentiating $4\pi T' = 8\pi P - z^{-2} + 3Q^2 z^{-4}$ gives

$$4\pi T'' = 2z^{-3} - 12Q^2 z^{-5}, \qquad 4\pi T''' = -6z^{-4} + 60Q^2 z^{-6}.$$

With $Q^2 = r_c^2/6$, these expressions give $T''(r_c) = 0$ and $T'''(r_c) = 1/(\pi r_c^4)$. In particular the temperature shift starts at cubic order in $z - r_c$.

More generally, set $\delta = z - z_0$, let $T' = \alpha\delta^m[1 + O(\delta)]$ with $\alpha \neq 0$, and assume $T_0 S_0' \neq 0$. Integration and division give

$$T - T_0 = A\delta^{m+1}[1 + O(\delta)], \quad A = \frac{\alpha}{m+1}, \qquad C_{P,Q} = \frac{T_0 S_0'}{\alpha}\delta^{-m}[1 + O(\delta)].$$

The analytic factor in brackets in the first expression equals one at $\delta = 0$. It has a holomorphic $(m+1)$st root there, so on any fixed inverse branch

$$\delta = \left(\frac{T - T_0}{A}\right)^{1/(m+1)} \left[1 + O\Big((T - T_0)^{1/(m+1)}\Big)\right].$$

Substitution into the heat capacity gives the leading power $-m/(m+1)$. A simple spinodal has $m = 1$ and exponent $-1/2$. The critical isobar has $m = 2$ and exponent $-2/3$.

Reduced roots and the contour count. Insert $z = r_c x$, $P = pP_c$ and $Q^2 = r_c^2/6$ in T/T_c. Since $8\pi P_c r_c^2 = 1/2$, differentiation gives

$$\tau_p = \frac{3}{4}\left(\frac{px}{2} + \frac{1}{x} - \frac{1}{6x^3}\right), \qquad \chi_p = \frac{3}{8}\left(p - \frac{2}{x^2} + \frac{1}{x^4}\right) = \frac{3}{8x^4}L_p(x), \qquad L_p(x) = px^4 - 2x^2 + 1.$$

Solving $L_p = 0$ as a quadratic in x^2 gives $x^2 = (1 \pm \sqrt{1-p})/p$. At $p = 3/4$ the positive roots are $\sqrt{2/3}$ and $\sqrt{2}$, with temperatures $3\sqrt{6}/8$ and $5\sqrt{2}/8$ in units of T_c. These are the maximum and minimum in Fig. 2. For comparison, $\tau_{3/4} = 0$ requires $9x^4 + 24x^2 - 4 = 0$, whose positive root is $x_e = \sqrt{(2\sqrt{5} - 4)/3} \simeq 0.39671$. At $p = 1$, $L_1 = (x-1)^2(x+1)^2$. At $p = 5/4$, $x^2 = (4 \pm 2i)/5$, giving the two roots with positive real part in Fig. 3.

Let x_j denote the distinct roots of L_p and m_j their multiplicities. Logarithmic differentiation yields the partial fractions

$$\frac{\chi_p'}{\chi_p} = \frac{L_p'}{L_p} - \frac{4}{x} = \sum_j \frac{m_j}{x - x_j} - \frac{4}{x}.$$

The circle $|x - 1| = 1/2$ excludes 0. For $3/4 \leq p \leq 1$, the expressions $x^2 = 1/(1 \mp \sqrt{1-p})$ place both positive roots between $\sqrt{2/3}$ and $\sqrt{2}$. For $1 < p \leq 5/4$, the roots with positive real part satisfy $|x^2 - 1|^2 = (p-1)/p \leq 1/5$ and $|x + 1| > 1$, so $|x - 1| < 1/2$. The left-half-plane partners stay outside. The enclosed residues therefore sum to two throughout this interval.

For a numerical check take $x = c + Re^{i\theta}$. Then $dx = i(x - c)d\theta$, and equispaced angles $\theta_k = 2\pi k/n$ give

$$W_n = \frac{1}{n}\sum_{k=0}^{n-1}(x_k - c)\frac{\tau_p''(x_k)}{\tau_p'(x_k)}, \qquad x_k = c + Re^{2\pi i k/n}.$$

At $p = 3/4$, $c = 1$, $R = 1/2$ and $n = 256$, numerical derivatives evaluated at 60 decimal digits give $|W_n - 2| \simeq 1.1833 \times 10^{-21}$. The same quadrature on a circle of radius $1/12$ about either simple positive root gives its unit residue. A circle of radius $1/4$ about 0 at $p = 5/4$ isolates the term $-4/x$ and returns index -4.

B.5 The two coexistence radii and the normalized curvature

Equal-temperature and equal-free-energy conditions. At fixed $Q \neq 0$ and $P > 0$, substitution of $T = (8\pi Pr + r^{-1} - Q^2 r^{-3})/(4\pi)$ and $S = \pi r^2$ gives

$$TS = 2\pi Pr^3 + \frac{r}{4} - \frac{Q^2}{4r},$$
$$G = M - TS = \left(\frac{r}{2} + \frac{Q^2}{2r} + \frac{4\pi P}{3}r^3\right) - \left(2\pi Pr^3 + \frac{r}{4} - \frac{Q^2}{4r}\right) = \frac{r}{4} + \frac{3Q^2}{4r} - \frac{2\pi P}{3}r^3.$$

Take two positive radii $a < b$ and write $s = a + b$, $v = ab$, and $h = a^2 + ab + b^2 = s^2 - v$. The divided differences are

$$\frac{a^{-1} - b^{-1}}{a - b} = -\frac{1}{ab} = -\frac{1}{v}, \qquad \frac{a^3 - b^3}{a - b} = h, \qquad \frac{a^{-3} - b^{-3}}{a - b} = -\frac{h}{a^3 b^3} = -\frac{h}{v^3}.$$

Thus $T(a) = T(b)$ and $G(a) = G(b)$ require

$$\frac{4\pi[T(a) - T(b)]}{a - b} = 8\pi P - \frac{1}{v} + \frac{Q^2 h}{v^3} = 0,$$
$$\frac{4[G(a) - G(b)]}{a - b} = 1 - \frac{3Q^2}{v} - \frac{8\pi P h}{3} = 0.$$

Eliminate $8\pi P$ between these equations and multiply by $3v^3$ to obtain

$$0 = hv^2 - Q^2 h^2 - 3v^3 + 9Q^2 v^2 = (h - 3v)\,[v^2 - Q^2(h + 3v)].$$

Since $h - 3v = (b - a)^2 > 0$ and $h + 3v = s^2 + 2v$, the second factor fixes

$$Q^2 = \frac{v^2}{s^2 + 2v}, \qquad 8\pi P = \frac{v^2 - Q^2 h}{v^3} = \frac{3Q^2}{v^2}, \qquad p = 96\pi Q^2 P = \frac{36Q^4}{v^2}.$$

Hence $v = 6Q^2/\sqrt{p}$ and $s = \sqrt{v^2/Q^2 - 2v}$. The radii are $(s \mp \sqrt{s^2 - 4v})/2$. Their discriminant is $v(v/Q^2 - 6)$, positive precisely for $0 < p < 1$. In this range $s > \sqrt{s^2 - 4v}$, which ensures that both radii are positive.

Temperature and stability of the two phases. Insert the coexistence values of P, Q^2 into the equation of state at $r = a$. Since $v = ab$,

$$\frac{4\pi v^3}{Q^2} T(a) = 3av + b(s^2 + 2v) - b^3 = 4a^2 b + 4ab^2 = 4vs,$$
$$T_* = \frac{Q^2 s}{\pi v^2} > 0.$$

The expression at b follows on interchanging the radii. With $T_c = 1/(3\sqrt{6}\,\pi|Q|)$, these relations give

$$\frac{T_*^2}{T_c^2} = \frac{54Q^6}{v^4}\left(\frac{v^2}{Q^2} - 2v\right) = \frac{54Q^4}{v^2}\left(1 - \frac{2Q^2}{v}\right) = \frac{3p}{2}\left(1 - \frac{\sqrt{p}}{3}\right).$$

The positive square root is Eq. (23) of Ref. [48]. As p tends to one from below, $v \to 6Q^2$, the discriminant vanishes and $a, b \to \sqrt{6}\,|Q|$. As p tends to zero from above, $T_*/T_c \sim \sqrt{3p/2}$.

The spinodal denominator is $D(r) = 4\pi r^4 T'(r) = 8\pi P r^4 - r^2 + 3Q^2$. At a it becomes

$$(s^2 + 2v)D(a) = 3a^4 - a^2(a^2 + 4ab + b^2) + 3a^2 b^2 = 2a^2(a - b)^2 > 0.$$

Interchanging a, b gives the result at b. Since $C_{P,Q} = TS'/T'$, both phases have finite positive heat capacity. One can compare their free energies with every positive radius in the same family. Let $k = 4\pi P/3$ and $G_* = G(a) = G(b)$. The coexistence relations give

$$Q^2/2 = kv^2, \qquad \pi T_* = 2ks, \qquad 1/2 = k(s^2 + 2v), \qquad G_* = 2ksv.$$

For the last coefficient, direct substitution gives

$$G(a) = \tfrac{k}{2}\left[(s^2 + 2v)a + 3v^2/a - a^3\right] = \tfrac{k}{2}(4a^2 b + 4ab^2) = 2ksv.$$

At bath temperature T_* the free-energy difference then factors as

$$r[M(r) - T_* S(r) - G_*] = kr^4 - \pi T_* r^3 + \tfrac{1}{2}r^2 - G_* r + \tfrac{1}{2}Q^2$$
$$= k(r^2 - sr + v)^2 = k(r - a)^2(r - b)^2.$$

The off-shell spherical family parametrized by $r > 0$ has exactly two global minima at this bath temperature, since $k/r > 0$ and the difference vanishes only at a, b.

From the temperature–volume metric to the isobaric response. Wei, Liu and Mann define $R_N = C_V R_{(T,V)}$ in Eq. (12) of Ref. [49], keeping C_V constant while taking the curvature. Their Eq. (13), with their curvature sign, uses the reduced thermodynamic volume $V/V_c = x^3$, where $x = r/r_c$ and $\tau = T/T_c$. Writing $L = 3x^2 - 1$ and $B_* = 2\tau x^3$, its numerator and denominator give

$$R_N = \frac{(3x^2-1)(3x^2-4\tau x^3-1)}{2(3x^2-2\tau x^3-1)^2} = \frac{L(L-2B_*)}{2(L-B_*)^2} = \frac{(L-B_*)^2 - B_*^2}{2(L-B_*)^2}.$$

The sign convention can also be checked before restricting to an isobar. With $C_V = c > 0$ constant, write the regulated fluctuation line element as $E\,dT^2 + J\,dV^2$, where $E = c/T^2$ and $J = -P_V/T$. Here pressure derivatives with respect to V are taken at fixed T, Q. Work first on a stable patch with $T > 0$ and $P_V < 0$, where $E, J > 0$. The resulting rational identity extends to regular branches with $P_V \neq 0$. Since $\partial_V E = 0$, the diagonal-metric curvature formula in Sec. 3 reduces to

$$cR^{\text{Sec. 3}}_{(T,V)} = -\frac{c}{\sqrt{EJ}}\partial_T\left(\frac{J_T}{\sqrt{EJ}}\right) = -\frac{T^2 J_{TT}}{J} - \frac{T J_T}{J} + \frac{T^2 J_T^2}{2J^2}.$$

The derivative here holds V, Q fixed. Since P is linear in T, write $P_V = AT + B$, with $A = P_{TV}$ and A, B independent of T. Substitution of $J = -A - B/T$, $J_T = B/T^2$, and $J_{TT} = -2B/T^3$ gives

$$\begin{aligned} cR^{\text{Sec. 3}}_{(T,V)} &= \frac{B}{TJ} + \frac{B^2}{2T^2J^2} = -\frac{B}{AT+B} + \frac{B^2}{2(AT+B)^2} \\ &= \frac{1}{2}\left[\left(\frac{TP_{TV}}{P_V}\right)^2 - 1\right]. \end{aligned}$$

The regulator cancels before the limit $c \to 0^+$. The scalar in Eq. (13) of Ref. [49] uses the opposite curvature sign, so $R_N = -cR^{\text{Sec. 3}}_{(T,V)}$ in this notation. Indeed, $P_T = 1/(2r)$, $P_{TV} = -1/(8\pi r^4)$, and $S_V = 1/(2r)$ give $S_V P_T/(2S) = -P_{TV}$. The isobaric derivative $(\partial_V T)_{P,Q} = -P_V/P_T$ then yields

$$\frac{C_{P,Q}}{2S} = \frac{TS_V}{2S(\partial_V T)_{P,Q}} = \frac{TP_{TV}}{P_V}.$$

Along an isobar the reduced temperature and its slope are

$$\tau_p(x) = \frac{3px^4 + 6x^2 - 1}{8x^3}, \qquad \tau_p'(x) = \frac{3(px^4 - 2x^2 + 1)}{8x^4}.$$

Substitution into $L - B_*$ yields

$$\begin{aligned} L - B_* &= 3x^2 - 1 - \frac{3px^4 + 6x^2 - 1}{4} = -\frac{3}{4}(px^4 - 2x^2 + 1) = -2x^4\tau_p', \\ \frac{B_*}{L - B_*} &= -\frac{\tau_p}{x\tau_p'}. \end{aligned}$$

Since $S = \pi r_c^2 x^2$, $dS/dx = 2S/x$ and $C_{P,Q} = \tau_p(dS/dx)/\tau_p'$. The squared ratio in R_N therefore equals $[C_{P,Q}/(2S)]^2$. At a simple zero x_s of τ_p', with positive temperature, its leading contribution is

$$R_N \sim -\frac{1}{2}\left[\frac{\tau_p(x_s)}{x_s\tau_p''(x_s)}\right]^2 (x - x_s)^{-2}.$$

For the two isobars of Fig. 4, put $\epsilon = r/r_0 - 1$ and use the dimensionless functions of Appendix A. At $p = 1$, $r_0 = r_c$, $K = 2\epsilon^2 + O(\epsilon^3)$ and $H = 4/3 + O(\epsilon)$, so

$$\frac{C_{P,Q}}{2S} \sim \frac{2}{3\epsilon^2} = \frac{2r_c^2}{3(r-r_c)^2} = \frac{4Q^2}{(r-r_c)^2},$$
$$R_N \sim -\frac{2}{9\epsilon^4} = -\frac{2r_c^4}{9(r-r_c)^4} = -\frac{8Q^4}{(r-r_c)^4},$$
$$\lim_{r\to r_c} \pi Q^2 R = \frac{1}{12}\frac{(2/3)(4/3+2/3)}{(4/3)(1/9)} = \frac{3}{4}.$$

At $p = 3$, $r_0 = r_*$, $H, K \to 1$ and $D_g = 2\epsilon^2 + O(\epsilon^3)$. Thus

$$\frac{C_{P,Q}}{2S} \to 1, \qquad R_N \to \frac{1-1^2}{2} = 0, \qquad \pi Q^2 R \sim \frac{3}{12}\frac{1}{(2\epsilon^2)^2} = \frac{1}{16\epsilon^4}.$$

References

[1] J. M. Bardeen, B. Carter, and S. W. Hawking, The four laws of black hole mechanics. *Communications in Mathematical Physics* **31**, 161–170 (1973). 10.1007/BF01645742.

[2] Jacob D. Bekenstein, Black holes and entropy. *Physical Review D* **7**, 2333–2346 (1973). 10.1103/PhysRevD.7.2333.

[3] S. W. Hawking, Particle creation by black holes. *Communications in Mathematical Physics* **43**, 199–220 (1975). 10.1007/BF02345020.

[4] J. B. Hartle and S. W. Hawking, Path-integral derivation of black-hole radiance. *Physical Review D* **13**, 2188–2203 (1976). 10.1103/PhysRevD.13.2188.

[5] G. W. Gibbons and S. W. Hawking, Action integrals and partition functions in quantum gravity. *Physical Review D* **15**, 2752–2756 (1977). 10.1103/PhysRevD.15.2752.

[6] K. Srinivasan and T. Padmanabhan, Particle production and complex path analysis. *Physical Review D* **60**, 024007 (1999). 10.1103/PhysRevD.60.024007.

[7] Maulik K. Parikh and Frank Wilczek, Hawking radiation as tunneling. *Physical Review Letters* **85**, 5042–5045 (2000). 10.1103/PhysRevLett.85.5042.

[8] L. Vanzo, G. Acquaviva, and R. Di Criscienzo, Tunnelling methods and Hawking's radiation: achievements and prospects. *Classical and Quantum Gravity* **28**, 183001 (2011). 10.1088/0264-9381/28/18/183001.

[9] Charles W. Robson, Leone Di Mauro Villari, and Fabio Biancalana, Topological nature of the Hawking temperature of black holes. *Physical Review D* **99**, 044042 (2019). 10.1103/PhysRevD.99.044042.

[10] Sang Pyo Kim, Hawking radiation as quantum tunneling in Rindler coordinate. *J. High Energy Phys.* **11**, 048 (2007). 10.1088/1126-6708/2007/11/048.

[11] Wen-Xiang Chen and Yao-Guang Zheng, Calculating the Hawking temperatures of Kerr–Newman black holes in the f(R) gravity models with the RVB method. *International Journal of Modern Physics A* **40**, 2550077 (2025). 10.1142/S0217751X25500770.

[12] Wen-Xiang Chen, Calculating the Hawking temperature of black holes in f(Q) gravity using the RVB method: a residue-based approach. *Canadian Journal of Physics* **103**, 531–542 (2025). 10.1139/cjp-2024-0214.

[13] Wen-Xiang Chen, Horizon residues and test-scalar quasinormal modes of a perturbative Schwarzschild-type black hole in quadratic f(Q) gravity. *European Physical Journal C* **86**, 991 (2026). 10.1140/epjc/s10052-026-16260-4.

[14] Wen-Xiang Chen, *Higher-Dimensional Black Hole Hawking Temperature and Entropy from the RVB–Residue Method: Tangherlini–AdS and Einstein–Gauss–Bonnet Examples*. Cambridge Open Engage working paper, version 1 (2026). 10.33774/coe-2026-48jjt.

[15] Wen-Xiang Chen, *Geometry as Thermodynamics: Entropy Stationarity and Horizon Residues*. arXiv preprint, version 1 (2026). arXiv:2609.30660v1 [gr-qc].

[16] F. Weinhold, Metric geometry of equilibrium thermodynamics. *J. Chem. Phys.* **63**, 2479–2483 (1975). 10.1063/1.431689.

[17] G. Ruppeiner, Thermodynamics: A Riemannian geometric model. *Phys. Rev. A* **20**, 1608–1613 (1979). 10.1103/PhysRevA.20.1608.

[18] G. Ruppeiner, Riemannian geometry in thermodynamic fluctuation theory. *Rev. Mod. Phys.* **67**, 605–659 (1995). Erratum, Rev. Mod. Phys. 68, 313 (1996). 10.1103/RevModPhys.67.605.

[19] J. E. Åman, I. Bengtsson, and N. Pidokrajt, Geometry of black hole thermodynamics. *Gen. Relativ. Gravit.* **35**, 1733–1743 (2003). 10.1023/A:1026058111582.

[20] P. C. W. Davies, The thermodynamic theory of black holes. *Proc. R. Soc. Lond. A* **353**, 499–521 (1977). 10.1098/rspa.1977.0047.

[21] J. Shen, R.-G. Cai, B. Wang, and R.-K. Su, Thermodynamic geometry and critical behavior of black holes. *Int. J. Mod. Phys. A* **22**, 11–27 (2007). 10.1142/S0217751X07034064.

[22] H. Liu, H. Lü, M. Luo, and K.-N. Shao, Thermodynamical metrics and black hole phase transitions. *J. High Energy Phys.* **12**, 054 (2010). 10.1007/JHEP12(2010)054.

[23] S. A. Hosseini Mansoori, B. Mirza, and M. Fazel, Hessian matrix, specific heats, Nambu brackets, and thermodynamic geometry. *J. High Energy Phys.* **04**, 115 (2015). 10.1007/JHEP04(2015)115.

[24] Banks, Tom, Linda M. Carpenter, and J-F. Fortin. "Undetected Higgs decays and neutrino masses in gauge mediated, lepton number violating models." Journal of High Energy Physics 2008.09 (2008): 087-087.

[25] G. Ruppeiner, Thermodynamic curvature and phase transitions in Kerr–Newman black holes. *Phys. Rev. D* **78**, 024016 (2008). 10.1103/PhysRevD.78.024016.

[26] H. Quevedo, Geometrothermodynamics. *J. Math. Phys.* **48**, 013506 (2007). 10.1063/1.2409524.

[27] Wen-Xiang Chen and Yao-Guang Zheng, Thermodynamic geometric analysis of RN black holes under f(R) gravity. *Canadian Journal of Physics* **104**, 1–27 (2026). 10.1139/cjp-2025-0237.

[28] Shao-Wen Wei, Yu-Xiao Liu, and Robert B. Mann, Black hole solutions as topological thermodynamic defects. *Phys. Rev. Lett.* **129**, 191101 (2022). 10.1103/PhysRevLett.129.191101.

[29] Chaoxi Fang, Jie Jiang, and Ming Zhang, Revisiting thermodynamic topologies of black holes. *J. High Energy Phys.* **01**, 102 (2023). 10.1007/JHEP01(2023)102.

[30] Zhen-Ming Xu, Yu-Shan Wang, Bin Wu, and Wen-Li Yang, Generalized Maxwell equal area law and black holes in complex free energy. *Phys. Lett. B* **850**, 138528 (2024). 10.1016/j.physletb.2024.138528.

[31] Yu-Shan Wang, Zhen-Ming Xu, and Bin Wu, Thermodynamic phase transition and winding number for the third-order Lovelock black hole. *Chin. Phys. C* **48**, 095101 (2024). 10.1088/1674-1137/ad53ba.

[32] F. Barzi, H. El Moumni, and K. Masmar, Riemann surfaces and winding numbers of Rényi phase structure of charged-flat black holes. *Eur. Phys. J. C* **84**, 1141 (2024). 10.1140/epjc/s10052-024-13511-0.

[33] Shi-Hao Zhang, Shao-Wen Wei, Jing-Fei Zhang, and Xin Zhang, Unifying topological, geometric, and complex classifications of black hole thermodynamics. *Phys. Lett. B* **880**, 140822 (2026). 10.1016/j.physletb.2026.140822.

[34] Zhen-Ming Xu and Robert B. Mann, Thermodynamic supercriticality and complex phase diagram for the AdS black hole. *Phys. Rev. Lett.* **136**, 041402 (2026). 10.1103/c39y-zcz6.

[35] Robert M. Wald, Black hole entropy is the Noether charge. *Physical Review D* **48**, R3427–R3431 (1993). 10.1103/PhysRevD.48.R3427.

[36] Vivek Iyer and Robert M. Wald, Some properties of the Noether charge and a proposal for dynamical black hole entropy. *Physical Review D* **50**, 846–864 (1994). 10.1103/PhysRevD.50.846.

[37] James W. York, Jr., Black-hole thermodynamics and the Euclidean Einstein action. *Physical Review D* **33**, 2092–2099 (1986). 10.1103/PhysRevD.33.2092.

[38] G. W. Gibbons and R. E. Kallosh, Topology, entropy, and Witten index of dilaton black holes. *Physical Review D* **51**, 2839–2862 (1995). 10.1103/PhysRevD.51.2839.

[39] Jorma Louko and Stephen N. Winters-Hilt, Hamiltonian thermodynamics of the Reissner–Nordström–anti-de Sitter black hole. *Phys. Rev. D* **54**, 2647–2663 (1996). 10.1103/PhysRevD.54.2647.

[40] Andrew Chamblin, Roberto Emparan, Clifford V. Johnson, and Robert C. Myers, Holography, thermodynamics, and fluctuations of charged AdS black holes. *Phys. Rev. D* **60**, 104026 (1999). 10.1103/PhysRevD.60.104026.

[41] S. W. Hawking and Don N. Page, Thermodynamics of black holes in anti-de Sitter space. *Commun. Math. Phys.* **87**, 577–588 (1983). 10.1007/BF01208266.

[42] Andrew Chamblin, Roberto Emparan, Clifford V. Johnson, and Robert C. Myers, Charged AdS black holes and catastrophic holography. *Phys. Rev. D* **60**, 064018 (1999). 10.1103/PhysRevD.60.064018.

[43] David Kastor, Sourya Ray, and Jennie Traschen, Enthalpy and the mechanics of AdS black holes. *Class. Quantum Grav.* **26**, 195011 (2009). 10.1088/0264-9381/26/19/195011.

[44] Brian P. Dolan, Pressure and volume in the first law of black hole thermodynamics. *Class. Quantum Grav.* **28**, 235017 (2011). 10.1088/0264-9381/28/23/235017.

[45] David Kubizňák and Robert B. Mann, P–V criticality of charged AdS black holes. *J. High Energy Phys.* **07**, 033 (2012). 10.1007/JHEP07(2012)033.

[46] Li-Hua Wang, Yun He, and Meng-Sen Ma, Fractional phase transitions of RN-AdS black holes at their Davies points. *Chinese Physics C* **47**, 035102 (2023). 10.1088/1674-1137/aca957.

[47] Elias M. Stein and Rami Shakarchi, *Complex Analysis*. Princeton Lectures in Analysis, Vol. II, Princeton University Press (2003). ISBN 9780691113852.

[48] Shan-Quan Lan, Jie-Xiong Mo, and Wen-Biao Liu, A note on Maxwell's equal area law for black hole phase transition. *Eur. Phys. J. C* **75**, 419 (2015). 10.1140/epjc/s10052-015-3641-0.

[49] S.-W. Wei, Y.-X. Liu, and R. B. Mann, Repulsive interactions and universal properties of charged anti–de Sitter black hole microstructures. *Phys. Rev. Lett.* **123**, 071103 (2019). 10.1103/PhysRevLett.123.071103.

[50] S.-H. Zhang, J.-F. Zhang, and X. Zhang, *Thermodynamic geometry as the missing link: toward a unified framework for black hole first-order phase transitions*. arXiv preprint, version 1 (2026). arXiv:2609.31144v1 [gr-qc].

[51] C. Niu, Y. Tian, and X.-N. Wu, Critical phenomena and thermodynamic geometry of Reissner–Nordström–anti-de Sitter black holes. *Phys. Rev. D* **85**, 024017 (2012). 10.1103/PhysRevD.85.024017.

[52] P. Chaturvedi, S. Mondal, and G. Sengupta, Thermodynamic geometry of black holes in the canonical ensemble. *Phys. Rev. D* **98**, 086016 (2018). 10.1103/PhysRevD.98.086016.

[53] Shan-Ping Wu, Si-Jiang Yang, and Shao-Wen Wei, Extended thermodynamical topology of black hole. *European Physical Journal C* **85**, 1372 (2025). 10.1140/epjc/s10052-025-15098-6.

[54] T. D. Lee and C. N. Yang, Statistical theory of equations of state and phase transitions. II. Lattice gas and Ising model. *Phys. Rev.* **87**, 410–419 (1952). 10.1103/PhysRev.87.410.